DIMENSIONAL ANALYSIS OF 17 DOF RAILWAY VEHICLE SUSPENSION MODEL

MOHAMED FIKHRIE BIN ALIAS

A report submitted
In fulfillment of the requirement for the degree of
Bachelor of Mechanical Engineering

Faculty of Mechanical Engineering
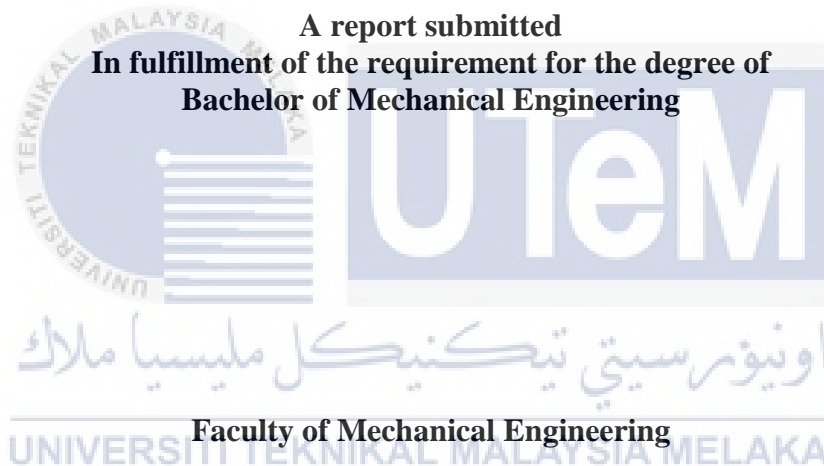
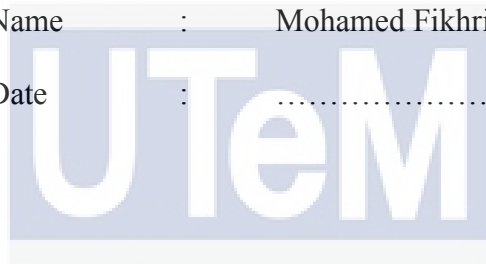## UNIVERSITI TEKNIKAL MALAYSIA MELAKA

2019

DECLARATION

I declare that this project report entitled "Dimensional analysis of 17 railway vehicle suspension model" is the result of my own work except as cited in the references

Signature   :   ……………………………

Name   :   Mohamed Fikhrie bin Alias
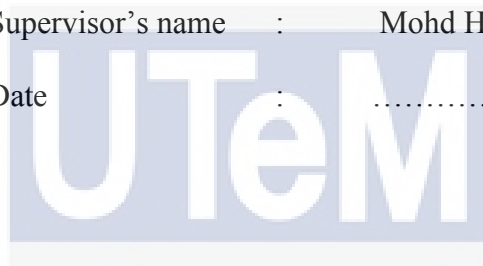
Date   :   …………………………

APPROVAL

I hereby declare that I have read this project report and in my opinion this report is sufficient in term of scope and quality for the award of the degree of Bachelor of Mechanical Engineering.

Signature   :   ……………………..

Supervisor's name   :   Mohd Hanif bin Harun

Date   :   ……………………..…

DEDICATION

To my beloved parents, supervisor and friends

ABSTRACT

Dimensional analysis is method that used to convert one unit to another unit. It is very important to understand the physical nature of the problem. In the railway vehicle lateral model, dimensional analysis is described as one of the best way to analyze the performance of the railway vehicle in the real and small scale. On the first part of the study, the dynamic modelling of full railway vehicle is used to perform the dimensional analysis in order to observe the acceleration, roll and yaw of the railway vehicle. The full railway vehicle model consist of 17 degree of freedom were described. In particular, one of the objective of the study was to determine the dimensional analysis based on the scaling method. The simulation software, MATLAB Simulink also were studied as one of the medium to analyzed several graph from the simulation work such as body displacement, body acceleration, body yaw angle and body rolling angle. For the second part of the study, the validation between the simulation models were done. To achieve this, the experimental result for the railway vehicle behavior were applied using a simple mechanism to study the pattern and also the performances of both simulation and experiment model. The discussion were including the analysis of the validation and the behavior of the railway vehicle.

ABSTRAK

Kajian kepada dimensi merupakan salah satu cara untuk menukarkan satu unit kepada unit yang lain. Ia sangat penting untuk memahami sifat fizikal kepada masalah. Dalam model sisi kereta api, analisis dimensi digambarkan salah satu kaedah yang terbaik untuk menganalisis prestasi model kereta api dalam skala yang sebenar dan kecil. Dalam bahagian pertama kajian PSM ini, model penuh kepada dinamik kereta api digunakan untuk melakukan dimensi analisis untuk mengkaji pecutan, gulingan dan ayakan model kereta api. Model kenderaan kereta api yang terdiri daripada 17 darjah kebebasan diterangkan. Khususnya, salaha satu objektif kajian ini adalah untuk menentukan analisis dimensi berdasarkan kaedah skala. Perisian computer yang dikenali sebagai MATLAB- Simulink juga dipelajari sebagai salah satu medium untuk menganalisis beberapa graf dari kerja simulasi seperti sesaran jasad, pecutan jasad, sudut ayakan badan dan sudut gulingan badan. Untuk bahagian kedua kajian, pengesahan antara model simulasi telah dilakukan. Untuk mencapai matlamat ini, keputusan eksperiment untuk tingkah laku kenderaaan kereta api telah diambil menggunakan mekanisma yang mudah untuk mengkaji corak dan juga prestasi untuk kedua-dua simulasi antara eksperimen dan simulasi. Perbincangan termasuk analisis pengesahan dan tingkah laku kenderaan kerata api.

ACKNOWLEDGEMENTS

TABLE OF CONTENT

LIST OF TABLE

LIST OF FIGURE

TITLE	PAGE

LIST OF ABBREVATIONS

DOF	-	Degree of freedom
RCF	-	Rolling Contact Fatigue
FE	-	Finite Element
LRT	-	Light rail transport
FLC	-	fuzzy logic control

v

LIST OF SYMBOLS

M	-	Car body mass
J_ψ	-	Yaw inertia of car body
J_θ	-	Roll inertia of car body
Y	-	Lateral displacement of car body
ψ	-	Yaw angle of car body
θ	-	Roll angle of car body
M_1	-	Bogie mass
$J_{1\psi}$	-	Yaw inertia of bogie
$J_{1\theta}$	-	Roll inertia of bogie
Y_{1-2}	-	Lateral displacement of the frontal and back bogies
ψ_{1-2}	-	Yaw angle of the frontal and back bogies
θ_{1-2}	-	Roll angle of the frontal and back bogies
m_0	-	Mass of wheel sets

$J_{0\psi}$	-	Yaw inertia of wheel sets
Y_{m1-m4}	-	Lateral displacement of wheel sets
ψ_{m1-m4}	-	Yaw angles of wheel set
K_{1y}	-	Primary lateral stiffness per wheel set
$K_{1\psi}$	-	Primary yaw stiffness per wheel set
$K_{1\theta}$	-	Primary roll stiffness per wheel set
C_{1y}	-	Primary lateral damping per wheel set
$C_{1\psi}$	-	Primary yaw damping per wheel set
$C_{1\theta}$	-	Primary roll damping per wheel set
K_{2y}	-	Secondary lateral stiffness per bogie
$K_{2\psi}$	-	Secondary yaw stiffness per bogie
$K_{2\theta}$	-	Secondary roll stiffness per bogie
C_{2y}	-	Secondary lateral damping per bogie
$C_{2\psi}$	-	Secondary yaw damping per bogie
$C_{2\theta}$	-	Secondary roll damping per bogie
ξ_{1-4}	-	Lateral irregularity of track under wheel sets
ρ_{1-4}	-	Horizontal irregularity of track under wheel sets
F_1, F_2	-	Damping force of MR dampers

F_{11} - Longitudinal creep coefficient

F_{22} - Lateral creep coefficient

W - Axle mass

λ - Wheel set tire slope ratio

r_0 - Wheel set radius

b - Semi wheel set spacing

b_1 - Lateral semi-spacing of the damper

b_3 - Second vertical semi-spacing of the damper

b_4 - Second longitudinal semi-spacing of the damper

L - Distance between the central line of the bogie and vehicle body

L_1 - Semi wheel-wheel spacing

h_1 - Height from center of body mass to the upper line of second spring

h_2 - Height from center of the body mass to central lateral damper

h_3 - Height from the upper line of second spring to center of sprung mass of the bogie

h_4 - Height from the center of the sprung mass of bogie to the center line of wheel set

h_5 - Height from the center of sprung mass of bogie to central lateral damper

CHAPTER 1

INTRODUCTION

The introduction is including background of study, problem statement, project objective, project scope, project Gantt chart, and project outline

1.1   Background of Study

The railway vehicles that run along a track are one of the most engineering studies in the world (Polach & Iwnicki, 2006). The track irregularities caused during the operation of high-speed railways deepen the vibrations of the track and the surrounding soil. The objective of this project was to improve the control of the vibration of different track irregularities in railway vehicles.

In England, the first such system was designed to perform locomotive testing (Shen & Yin, 2006). The Test Rig has a high- power electric motor that moves the rig and it was a rather expensive system. The control and measurement system are also particularly in details. Trains running at high speed (300-350 km/h) placed a high demand on the alignment of the rail lines and in order to improve the alignment and the stability of the tracks, the other option such as the structure of the stiffness and the track had been decided (Bian et al 2015). The effect of vibration propagation is studied and mention in (Kouroussis, 2014). It mentions that different type of

trains and various modelling approaches are presented for the evaluation of dynamical 1characteristic caused by the wheel/rail irregularities. It computationally to measure and studying the behavior of the rail and the vehicle itself. For the economic reason, suggestion for field test had been made for test on the moving train but it will demand a high cost for the test.

The track irregularities generated during the running service of high-speed railway aggravate vibrations of the track and the surrounding ground environment. The problem of mechanical vibration control is generally caused by placing the suspension system between the source of the vibration and also the structure that need to be protected. All type of the moving vehicle like car, motorcycle, train and others produce vibration when moving. These vibrations reduce ride and handling and also dealing with the safety and driving comfort. The Test Rig concept were implemented to observe how the performance of the railway can reduce the problem. The Test Rig with a similar dynamic behavior in term of the damping, resonance of the chassis, wheel mass and nonlinearities were used as one of the instrument to see the real behavior of the railway vehicle.(Koch et al. 2010)

1.2 Problem Statement

One of the most complex dynamical system in engineering is the railway vehicle running along a track. The interaction between the non-conservative forces generate by the relative motion in contact area and also the wheel and rail involve both geometry of wheel tread and rail head makes the system more systematic and most complex. Usually the experiment/simulation that used to carry out for the railway is based on mathematical model. The model used were a

full-scale model. That means an experiment that carried out were used a real parameter for the railway vehicle. It's computationally to measure and studying the behavior of the railway vehicle itself. The real scale model also demands a high cost for the test. Besides that, the operation for the test also need more workers as the real-scale were a big operation and the system must be handled with skills. The safety also become one of the important parts when to handle a test especially with the changing of the control such as damper and also the rail of the railway vehicle.

Due to the problem stated, the scaling strategy were developed to make sure the experiment/ simulation can be done without harming anyone. 17 degree of freedom (DOF) were used based on mathematical model that consider ride performance of vehicle body. Based on that, a scaled model using scaling strategy were used as the Test Rig to represent the real measurement of the railway vehicle but in a small test to achieve the minimum parametric represent the real physical of the model.

1.3   Project Objective

The objectives of this project are:

i.   To describe a full railway vehicle model with 17 degree of freedom (DOF).

ii.   To determine a dimensional analysis of railway vehicle model based on Jaschinski, Iwnicki, Pascal, and Jaschinski modified methods.

iii.   To validate a simulation model with experimental model available in the laboratory

1.4 Project Scope

The scope of this project is to described a full railway vehicles parameter that are selected to represent the parameter of the railway vehicle suspension model and only ride analysis is performed in this study. A 17 degree of freedom scale railway vehicle model will be used to represent the railway vehicle lateral model. The study will use a MATLAB-Simulink for simulation work. MATLAB-Simulink is a computer design tools that are used to simulate the dynamics behavior and also evaluate the performance of the structure. The simulation study will be performed to study lateral performance of the full railway vehicle. Besides that, the experiment will be carried out using a Test Rig that available at the laboratory to study the performance of the actual railway vehicle based on scaling method. The simulation model and experiment model will be validate.
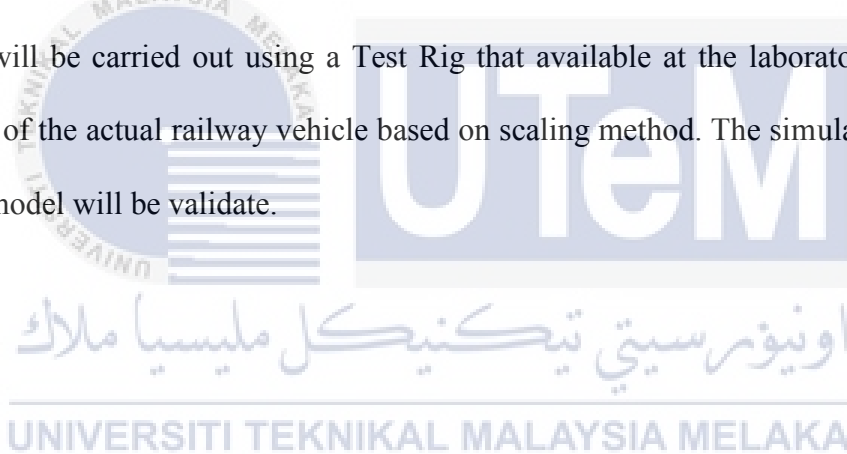
1.5 Project Outline

Chapter 1: The introduction including background, problem statement, project objective, project scope, and also project outline.

Chapter 2: the literature review consists of introduction, the history of small-scale railway vehicle, scaling strategy for 4 method used, pascal, iwnicki and jaschinski method, and also simulation model of railway vehicle for quarter car model, half car model and full car model.

4

Chapter 3: the research methodology is including development of 17-degree of freedom (DOF) of the full railway vehicle model, equation of bogie dynamic, wheel set dynamic and also vehicle body dynamic. The briefing about MATLAB Simulink is used as the additional study in this research. The briefing also about the experiment that carried out with the mechanism and also the sensor used.

Chapter4: in result and analysis, the PSM work will cover on the simulation result for the real scale of the railway vehicle and also the method used which is the small scale of the railway vehicle. The simulation work is done by using the MATLAB Simulink software. From the simulation, the graph of the displacement, acceleration, yaw and roll of the railway vehicle had been studied and analyzed. The validation result of the simulation and the experiment also analyzed and studied.

Chapter 5: the conclusion, summary and the recommendation for future study of the PSM work.

1.6   Summary
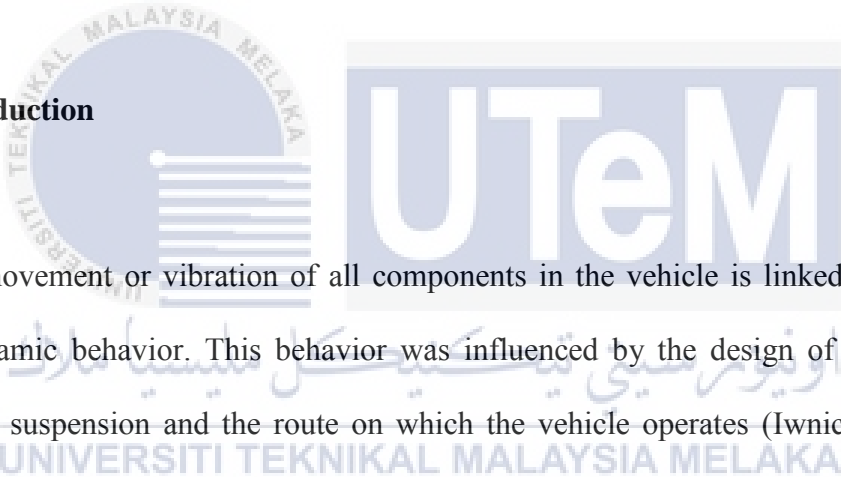
The main objectives of this study are to describing a full model of scale model with 17 DOF that consider ride performance of the vehicle. The study also proposes to select a scaling strategy through a simulation studies using MATLAB Simulink and determined the dimensional analysis using the scaling strategy. Lastly, the study will validate the simulation and the experiment model.

CHAPTER 2

LITERATURE REVIEW

The literature review consist introduction, the history of the small-scale vehicle, scaling strategy, Jaschinski method, Pascal method, Iwnicki method, Jaschinski modified method, and overview of simulation model of railway vehicle.

2.1   Introduction

The movement or vibration of all components in the vehicle is linked to the railway vehicle's dynamic behavior. This behavior was influenced by the design of the vehicle, in particular the suspension and the route on which the vehicle operates (Iwnicki & Wickens, 1998). It has indication for the relief of passengers or damage to things, for wheel and rail wear and noise era and for the protection of the railway device. One of the complex studies in engineering was the railway vehicle that running on the track. It is because the interaction between railway vehicle wheel and rail involves both complex geometry of wheel tread and rail head and also non-conservatives forces that generated by relative motion in the contact area. Improvement in rail material results in mitigating maintenance expenses and preventing the rail degradation triggered via rolling contact fatigue (RCF), which is occurred with the aid of the repeated rolling contact of wheels on rail (Naeimi et al. 2014). As claim by (C. Esveld, 2001), the highest stress level occurs at the running surface of the rail.

The track and the switches need to enable easy passage of the trains. If the track is no longer perfectly levelled and aligned, oscillation or vibration of the train will happen because of the irregularities of track (Dahlberg, 2006). Environment, Oscillations, vibrations, and noise can also grow to be disagreeable for the train passenger. Baiasu et al. (2013) mentioned that from (Sebesan et al. 2011) say that in view of the study of the vehicle's response in a horizontal plan, a mathematical model was developed that simulates the lateral dynamics of a four- axle railway vehicle. Zhou explained in his paper that he evolve the tilting control system that provide a comfortable response during curve and maintain the straight track ride (Zhou et al, 2011) but his method only for a real scale of the railway vehicle. The test rig is advantageous because its cost is not very high and its size is quite small. Generally speaking, all tests carried out on a bench are influenced by real behavior differences (Politecnico, 2000).

Figure 2. 1 : The test Rig (Guchi and Metin, 2009)

2.2   History of Small-Scale Railway Vehicle

In the late 18th and early 19th century, development of railway is concentrated on the prime mover and possibility of traction using adhesion but the major problem from the development was strength of material. The earliest vehicle used element of suspension adopted from horse carriage practice as the dynamic applied to the track were concern (Wickens, 2006). Many researchers have applied certain linear and non- linear control methods to rail vehicle models in the last decade. Rao and Prahlad (1997) applied a tunable FLC to suspension systems for vehicles. Metin & Guclu (2011) mentioned that a semi- active damping system was developed by (Stribersky et al. 1998) to reduce lateral acceleration. They therefore improve the convenience of a railway vehicle.

Guclu and Metin (2009) have modeled the Istanbul rail vehicle system as 22 DOF half light rail transport(LRT). Real parameters for the model vehicle were used in the simulation. FLC was used to actively control vibrations in the simulation environment to minimize the displacement and acceleration of the vibrations obtained at the end of simulations based on time and frequency domain. The historical backdrop of model trains extends back about 150 years, nearly as old as the railroad business itself. The main models were not developed to any one scale or standard, as were more similar to toys with no approach to have different trains.
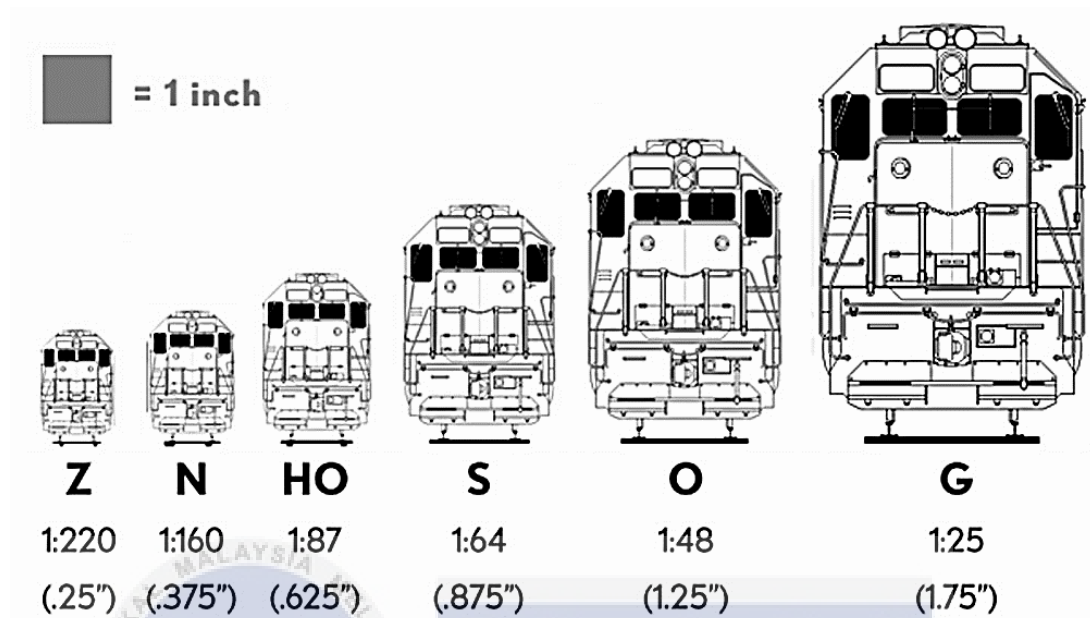
Figure 2. 2: Common Scale Used in railway vehicle (Craftman, 2016)

Scales were produced by side interest gatherings and devotees over the globe. They came up a unit of estimation that would relate between the model and the full measured, operational train. The historical backdrop of the creation and selection of these scales, is a history as interesting as the development of the model trains themselves. The scale model of the railway vehicle was developed by Lehmann Grosse Bahn in the 1960s (Craftman, 2016). The scale model was called G scale train and it was a toy that developed for fun. Before Lehmann, there is a time period between the first and second World Wars saw the rise of smaller model trains starting with S scale in the 1030s that developed by A.C. Gilbert Co (micro-mark, n.d.). The scale model looks more realistic looking two-rail track and becomes popular in that era. Then the smallest practical model railroading scale were designed by Marklin in Germany. It was called Z scale model and were developed in 1972 (Craftman, 2016).

1979 and 1982, the first experiment utilizing scaled models of railroad vehicles on scaled tracks were performed by Sweet at Princeton University. Trials were concerned about the mechanics of wrecking of progressively scaled 1/5 model of a typical three-piece cargo truck configuration generally used in North America (Grant et al., 2012). This study were supported by (Ji, Yamada, 1998) that used Sweet Parker scaled model in investigate a magnetic reconnection in controlled laboratory plasma. The power was scaled by similarity laws, including gravitation, the impact of inertia, spring stiffness, creep, and dry friction. This method had been currently used in many adopted scaling strategies.

2.3   Scaling Strategy

The scaling strategy is one of the most important aspects of the rig's design. It is guarantees that the chose parameters are effectively related and obey laws of similarities (Naeimi et al., 2014). The design of the scaling is evolved from rig concept, roller rig and also the track determined. This study also mentioned in the (Grant et al., 2012) saying that the dimension aspect of the new test rig determine the specification and the parameter of the system.

$$scaling\ parameter = \frac{real\ parameter}{scale} \tag{1}$$

There are different methodologies accessible to scaling. Before, it used method of dimensional analysis to establish the scaling factor that could be derived for each parameter (C. Heliot, 1986). There are also study that derived the equations of motion and then calculate the scaling factor to maintain the similarities (Iwnicki & Wickens, 1998). As discussed in (C. Heliot, 1986). A scaling strategy need to be selected based in the type of analysis that carried out in the test rig. There are three scaling method that considered in this study to determine which method is mostly exact with the real parameters proposed by Pascal, Iwnicki, and also Jaschinski.

2.3.1 Pascal's Method

It is suitable for practical and economic reasons for the construction of wheels and rollers with the same materials used in the wheel / rail system. The scaling factors of Yang and the module of density are uniform. The scaling factors of other physical dimensions can be achieved by simple formulas. The accelerations have a scaling factor equal to the inverse of the scaling length between the physical sizes. Gravity should also be changed on the model. In order to achieve this result, the contact force between wheel and rail is increased by simulating a body with a greater but equal weight by applying a normal force (Politecnico, 2000).

2.3.2 Iwnicki's Method

Apart from the dimension scaling factor, different scaling factors can be chosen in the construction of similarity laws. For these laws, Iwnicki takes a time-scale factor equal to one and the building material of wheel and rig is the same for similarity systems. This choice introduces a gravity scaling factor, but while the contact force between wheel and rail increases with the described laws (bigger mass with equal mass for increasing gravity), in this case it decreases. To increase the contact force a directed force is applied as gravity on the wheels, while the cables are used to reduce the gravity acceleration (Iwnicki & Wickens, 1998). It is intuitive that the change in gravity influences the dynamic behavior, but it is insignificant if the vehicle's lateral displacement is small.

2.3.3 Jaschinski's Method

Similarity studies are corrected in accordance with Reynolds if the exact scaling laws are taken into account for all physical sizes. In accordance with this principle, Jaschinski considers the simplified differential equations that describe the dynamics of the wheelset and the normal contact force between wheel and rail. In this way, several no-dimensional groups are obtained to extract the scaling factors. The scaling factor of the acceleration is unitary. The scaling factor of the creep force can be obtained either through motion equations or not through restriction equations, but the value should be the same (Eickhoff et al. 1995). Comparing the expression of the scaling factor of the creep force, a scaling factor of material density equal to the reverse of the scaling factor of the length is obtained. Jaschinski proposed two scaling methods as its very difficult to build obey this law, one for the dynamic study and the other for the study of wheel and rail contact (Jaschinski, 1990).

2.3.4 Jaschinski Modified's Method

The aim of the simulations is to evaluate the possibility of realizing a bogie test system on a curve with a constant radius. The scaling laws that introduce a gravity reduction factor are not suitable for this purpose. The methodology of Jaschinski does not allow the simultaneous study of contact and dynamic behavior. In order to eliminate this limit, a modification to the Jaschinski scaling laws was introduced (Politecnico, 2000). The main scaling factor for the physical dimensions used can be resumed as shown in Table I.

Table 1: List of scaling factor (Politecnico, 2000)

Scaling factors	Jaschinski	Pascal	Iwnicki	Jascinski modified
φ_l length	5	5	5	5
φ_t time	$\sqrt{5}$	5	1	$\sqrt{5}$
φ_V velocity	$\sqrt{5}$	1	5	$\sqrt{5}$
φ_a acceleration	1	1/5	5	1
φ_m mass	125	125	125	75
φ_F force	125	25	625	75
φ_ρ density	1	1	1	0.6
φ_E elastic module	1	1	1	3
φ_w weight	125	125	125	75
φ_C stiffness	25	5	125	15
φ_T creep force	125	25	625	75
φ_K damper	$25\sqrt{5}$	25	125	$15\sqrt{5}$
φ_{Ct} torsion stiffness	625	125	3125	375
φ_{Kt} torsion damper	$625\sqrt{5}$	625	3125	$375\sqrt{5}$
φ_I inertia	3125	3125	3125	1875
φ_μ friction	1	1	1	1

Table 2: Scaling factor of Kalker's coefficient (Kalker, 1973)

Scaling factors	MMU	Pascal	Jascinski $\rho = 1$	Jascinski $\rho = 0.5$	Jaschinski modified
f_{11}	73	25	125	125/2	40
f_{22}	73	25	125	125/2	40
f_{23}	625	125	625	625/2	80

2.4 Simulation Model of Railway Vehicle

2.4.1 Quarter Car Model

The quarter car model is consisting of a bogie and a set of wheels connected by primary suspension. The air spring is located between the body of the vehicle and the bogie, which includes an air bag connected to a surge reservoir through a control orifice (Oda, 1970). It also mentioned in (Islamic, 2016) saying that the active forces are being produced by the actuators when the active suspension is applied. The quarter car model is illustrated in figure below.
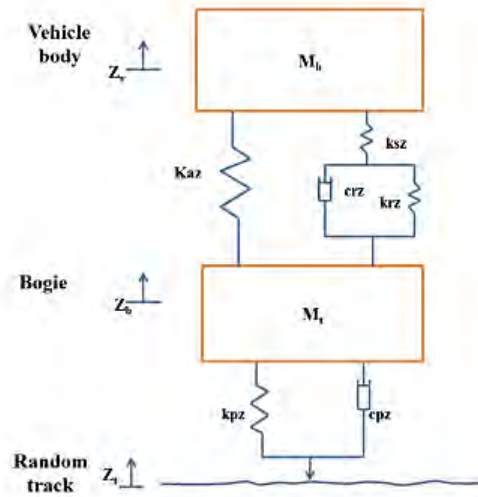

Figure 2. 3: The quarter car model of railway vehicle (Islamic, 2016)

The air spring model is modified by Oda and Nishimura in 1970, which has traditional air spring dynamics with an auxiliary reservoir. The primary suspensions and the track inputs are influenced by passive and active forces. Therefore, the forces acting on each mass can be used to model this system in order to create the motion equation of each mass.

The change of area stiffness k_a and the air spring mid-point mass m_{mp} has assumed to be zero because of their small value with respect to the total entire system. The general equation for air spring model can be written as,

$$c_{rz}\left(\dot{z}_b - \dot{z}_{mp}\right) + k_{rz}\left(z_b - z_{mp}\right) - k_{sz}\left(z_{mp} - z_v\right) = 0 \qquad (2.1)$$

Now after re-arranging the above equation it can be written as =

$$\dot{z}_{mp} = \frac{k_{rz}}{c_{rz}}z_v - \frac{k_{sz}-k_{rz}}{c_{rz}}z_{mp} + \frac{k_{rz}}{c_{rz}}z_b + \dot{z}_b \qquad (2.2)$$

Applying Newton s second law the equations of motion for the system are formulated. The equation of motion for the bounce of vehicle body (balancing force in z direction) can be represents,

$$\ddot{z}_v\, m_b = k_{sz}\left(z_{mp} - z_v\right) - k_{az}\left(z_b - z_v\right) \qquad (2.3)$$

After re-arranging, the equation is written as =

$$\ddot{z}_v = \frac{1}{m_b}\left(-(k_{az} + k_{sz})z_v + k_{sz}\,k_{mp} + k_{az}z_b\right) \qquad (2.4)$$

And the equation of bogie

$$\ddot{z}_b m_t = c_{pz}(\dot{z}_t - \dot{z}_b) + k_{pz}(z_t - z_b) + k_{sz}(z_{mp} - z_v) + k_{az}(z_b - z_v) \qquad (2.5)$$

or

$$\ddot{z}_b = \frac{1}{m_t}((k_{az} + k_{sz})z_v - k_{sz}k_{mp} - (k_{az} + k_{pz})z_b - c_{pz}\dot{z}_b + k_{pz}z_t + c_{pz}\dot{z}_t \qquad (2.6)$$

Equation 1 to 2 both are represent the system shown in the figure and can be arranged in a state-space form for system analysis and further controlled design.
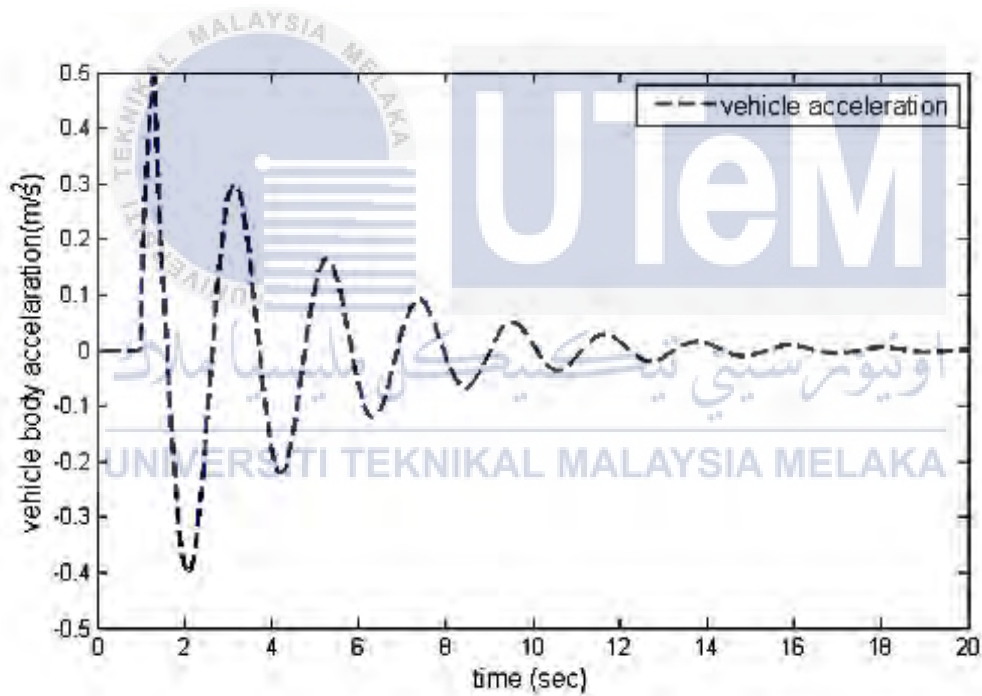

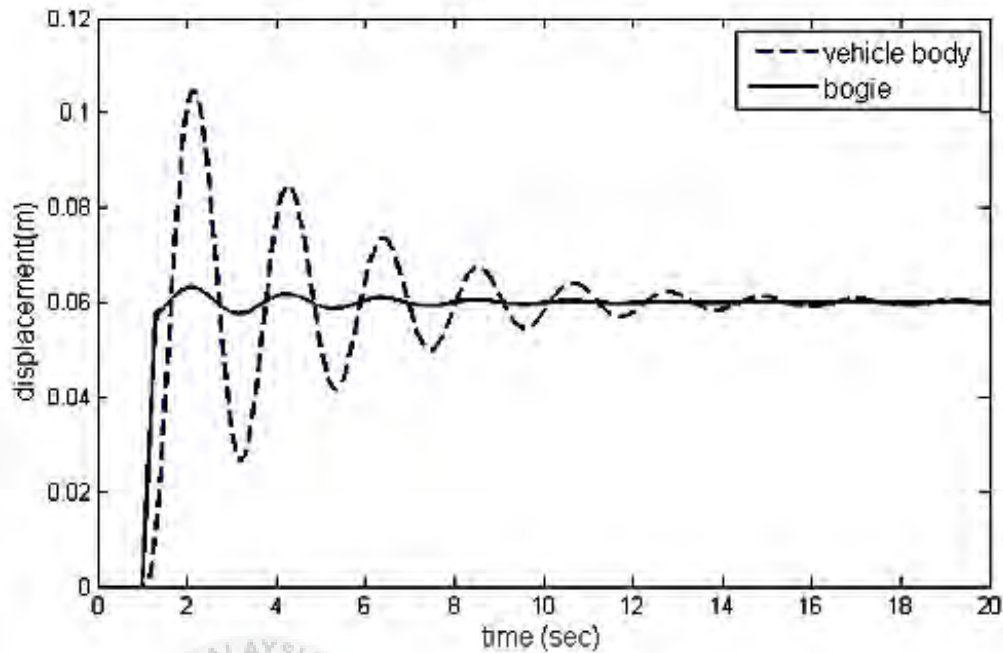Figure 2. 4: The vehicle body acceleration (Islamic, 2016)

16

Figure 2. 5: Vehicle and bogie displacement (Islamic, 2016)

The result show the graph of the vehicle body acceleration and also the vehicle and bogie displacement when the equation and the step track input were given. The simulation show the different graph of the real vehicle body from its acceleration and its displacement. The performance of the vehicle model had been assessed for random input which represent the misalignment of the rail track.

2.4.2   Half car model

Depending on the type of vehicle, structural shapes of vehicles can be quite complicated. The half car model can be studied in the (Shimamune & Tanifuji, 1995). That paper study about the application of oil-hydraulic actuator for railway suspension using half vehicle model. The model use 3-DOF half car which has three freedom of motion as bogie lateral, car body lateral and also car body roll.
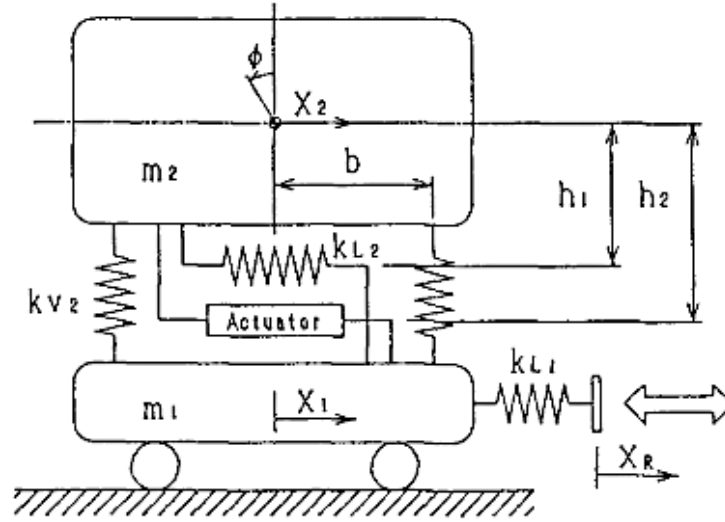
17

Figure 2. 6: Analytical model of half-vehicle model (Shimamune & Tanifuji, 1995)

The equation from the 3-DOF can be represent by

$$m_1\ddot{x}_1 - k_{L2}(x_2 + h_1\phi - x_1) + k_{L1}x_1 = A_s p + k_{L1}x_R \qquad (1)$$

$$m_2\ddot{x}_2 - k_{L2}(x_2 + h_1\phi - x_1) = A_s p \qquad (2)$$

$$I\ddot{\phi} - k_{L2}h_1(x_2 + h_1\phi - x_1) + k_{v2}b^2\phi = A_s ph_2 \qquad (3)$$

where m_1, is bogie mass, m_2 car body mass and I roll moment of inertia of car body. k_{L1} denotes primary lateral stiffness, k_{L2} secondary lateral stiffness and k_{v2} secondary vertical stiffness per bogie, respectively. 2b is spacing between the secondary vertical springs, hi height from secondary lateral spring to car body of gravity(CG), h_2 height from actuator to CG. A_s is cross-sectional area of actuator piston and p differencia1 pressure between cylinder chambers.

2.5   Summary

Chapter 2 presented a history of the small-scale railway vehicle with a bit description on how it develops. It also presented a on a first experiment/simulation that involving scaling strategy. The scaling strategy that used in this study also discussed in chapter 2 as four method were introduced. The previous simulation on the quarter car model and also half car model also presented in this chapter. It shows on how the modelling were develop and also the result in the simulation to show the different between the studies.

CHAPTER 3

METHODOLOGY

3.0 Introduction

This chapter discuss in details about the method used for modelling, the suspension system and the simulation process. This chapter started with a brief explanation of the step involved in this project followed by a methodology flowchart as the summary. The processes are described and discussed thoroughly in this chapter.

3.1 Modelling Assumption

The modelling assumption of this project are as follow:

I. Aerodynamic drag force is neglected

II. Rolling resistance due to anti roll bar and body flexibility are also neglected

III. The vehicle body, bogie and wheel-set are considered as rigid

IV. The suspension component between vehicle body and bogies are modelled as passive secondary suspension system consist of springs and dampers positioned in vertical, lateral and longitudinal directions. While the component between the bogies and wheel-set are modelled as passive primary suspension system.

V. The railway vehicle body is assumed to travel in longitudinal direction with constant speed.

VI. The wheel-set move along a straight rail at certain constant velocity with track alignment irregularity in a regarded as the external excitation to the railway vehicle system.
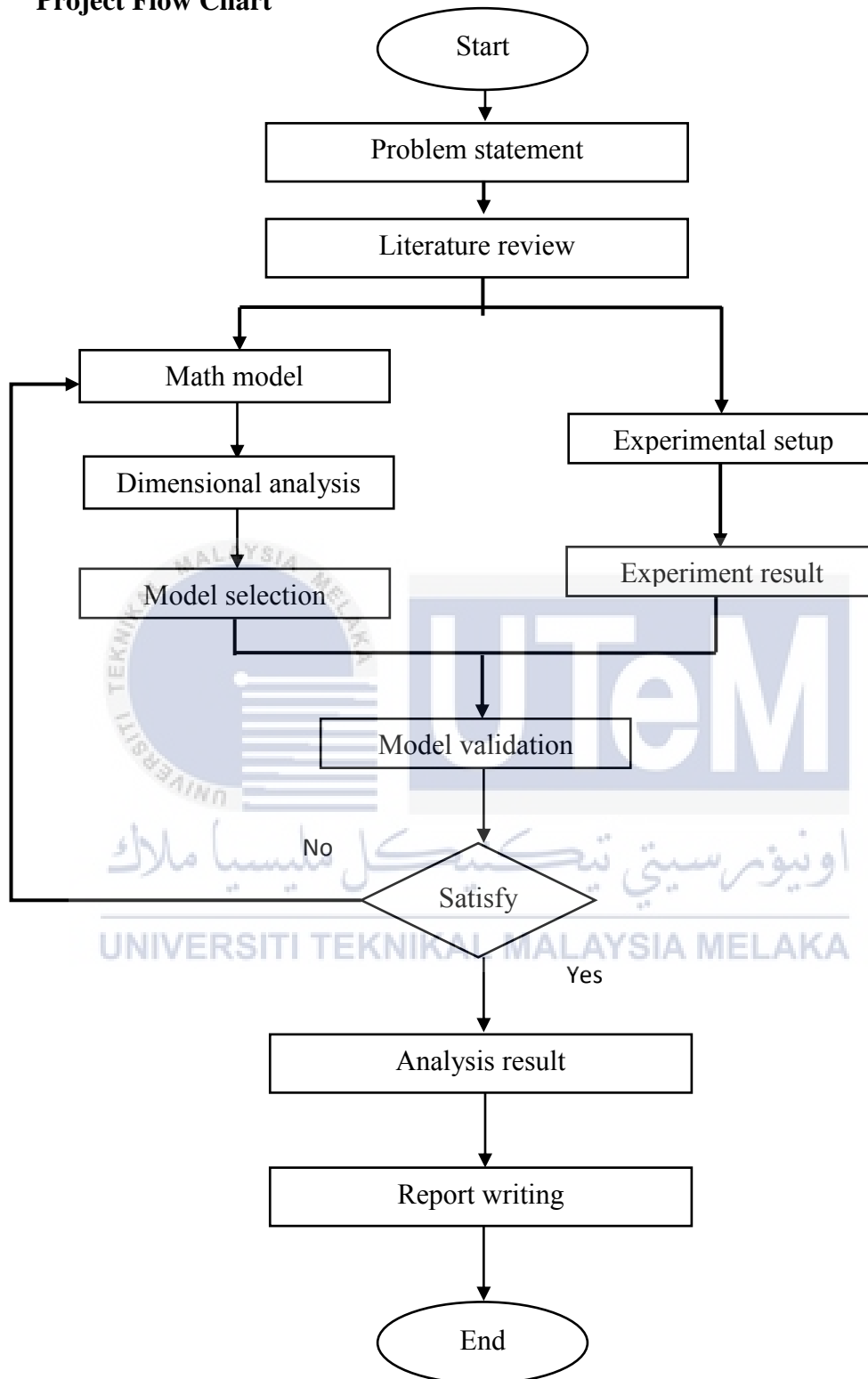
3.2   Project Flow Chart

Figure 3. 1 : Project Flowchart

3.2.1 FLOWCHART

The project were started with the 17 DOF of the railway vehicle model that consider ride performance of the vehicle body. A 17 DOF equation will represent the railway vehicle lateral model. The small scaling method such as Jaschinski, Pascal, Iwnicki and Jaschinski Modified were studied to come out with the dimensional analysis of the full scale and small scale. The input for the dimensional analysis were from a sine wave analysis.

17 DOF equation that represent the bogie dynamic, wheel set dynamic and also vehicle dynamic body were set in the MATLAB SIMULINK to came out with the modelling model. The modelling model will represent each of the scaling method and came out with a graph of the displacement, acceleration, roll angle and also yaw angle. The purpose to come out the graph were to identify how the pattern of the graph for each scaling method represented. From that, the small scale graph will be compared with the real scale graph to choose the best graph that will represent the small scaling method.

For the experimental setup, the Test Rig were introduced to come out with the actual analysis of the simulation. The Test Rig were occupied with the mechanism that were designed using a SOLIDWORK software and fabricated it. Then, it also occupied with the three sensor that is, LVDT sensor, gyro sensor, and also accelerometer. This sensor were placed to get the data from the experiment. This data using a random input were put into the simulation. From that, the model validation can be done from the model selection and also the experiment. If the validation were not satisfy, the math model will be adjusted. Otherwise, the full analysis of the result can be done.

3.3   17-DOF Railway Vehicle Dynamic Model

The model of the railway vehicle considered in this study consists of a vehicle body connected by two bogie masses to four-wheel sets and is represented as a 17-DOF. The body and bogie masses of the vehicle can roll and yaw and move in a lateral direction.

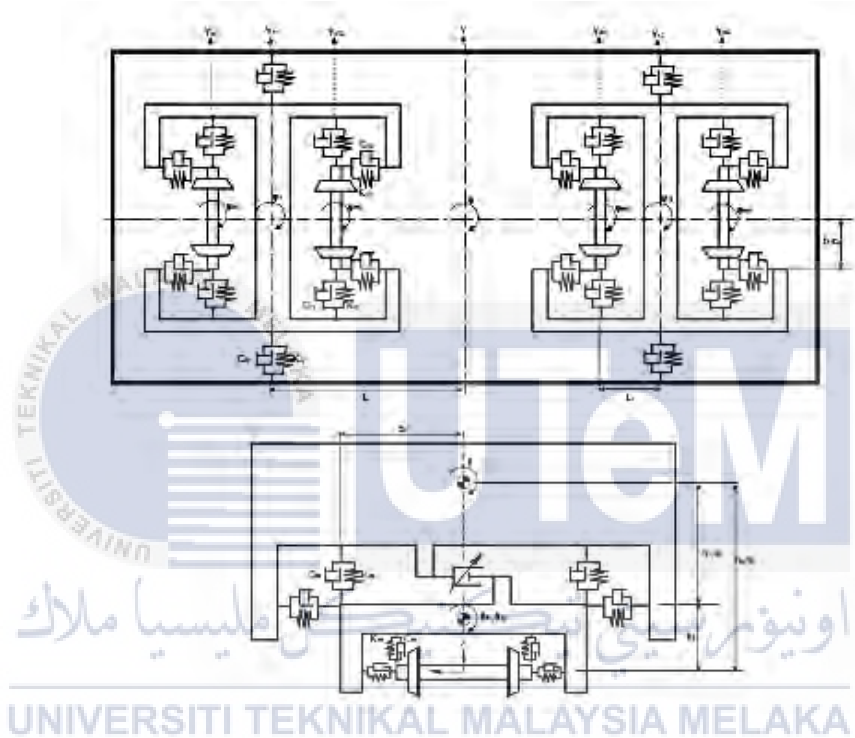Figure 3. 2: The plain view of 17-DOF railway vehicle model (Hudha et al. 2011)

Figure 3.1 shows the view of the 17-DOF railway model vehicle lateral suspension system. The motion equations for the 17 DOF were derived from the laws of Newton and the same model was used Hudha et al. (2011) and also (Ma & Yang, 2008). From the Newtonian method of dynamics, equations of motions of the model can be expressed as Equation (1)-(17).

3.3.1 Bogie Dynamic

Equations of motion for the two bogies in lateral direction:

$$M_1\ddot{Y}_{11} - 2K_{1y}(Y_{m1} + Y_{m2} - 2Y_{11} - 2h_4\theta_{11}) - 2C_{1y}(\dot{Y}_{m1} + \dot{Y}_{m2} - 2\dot{Y}_{11} - 2h_4\dot{\theta}_{11})$$

$$+2k_{2y}(Y_{11} - Y - h_3\theta_{11} - L\psi - h_1\theta) + 2C_{2y}(\dot{Y}_{11} + \dot{Y} - h_5\dot{\theta}_{11} - L\dot{\psi} - h_2\dot{\theta}) - F_1 = 0 \quad (3.1)$$

$$M_1\ddot{Y}_{12} - 2K_{1y}(Y_{m3} + Y_{m4} - 2Y_{12} - 2h_4\theta_{12}) - 2C_{1y}(\dot{Y}_{m3} + \dot{Y}_{m4} - 2\dot{Y}_{12} - 2h_4\dot{\theta}_{12})$$

$$+2k_{2y}(Y_{12} - Y - h_3\theta_{12} - L\psi - h_1\theta) + 2C_{2y}(\dot{Y}_{12} + \dot{Y} - h_5\dot{\theta}_{12} - L\dot{\psi} - h_2\dot{\theta}) - F_2 = 0 \quad (3.2)$$

Equation of motion for two bogies in yaw direction:

$$J_{1\psi}\ddot{\psi}_{11} - 2K_{1\psi}(\psi_{m1} + \psi_{m2} - 2\psi_{11}) - 2C_{1\psi}(\dot{\psi}_{m1} + \dot{\psi}_{m2} - 2\dot{\psi}_{11}) + 2k_{2\psi}(\psi_{11} - \psi)$$

$$+ 2C_{2\psi}(\dot{\psi}_{11} + \dot{\psi}) - 2K_{1y}L_1(Y_{m1} - Y_{m2} - 2L_1\psi_{11}) - 2C_{1y}L_1(\dot{Y}_{m1} + \dot{Y}_{m2} - 2L_1\dot{\psi}_{11})$$

$$-F_1b_4 = 0 \quad (3.3)$$

$$J_{1\psi}\ddot{\psi}_{12} - 2K_{1\psi}(\psi_{m3} + \psi_{m4} - 2\psi_{12}) - 2C_{1\psi}(\dot{\psi}_{m3} + \dot{\psi}_{m4} - 2\dot{\psi}_{12}) + 2k_{2\psi}(\psi_{12} - \psi)$$

$$+ 2C_{2\psi}(\dot{\psi}_{12} + \dot{\psi}) - 2K_{1y}L_1(Y_{m3} - Y_{m4} - 2L_1\psi_{12}) - 2C_{1y}L_1(\dot{Y}_{m3} + \dot{Y}_{m4} - 2L_1\dot{\psi}_{12})$$

$$-F_2b_4 = 0 \quad (3.4)$$

Equation of motion for two bogies in roll direction:

$$J_{1\theta}\ddot{\theta}_{11} - 4K_{1\theta}\theta_{11} + 4C_{1\theta}\dot{\theta}_{11} - 2K_{2y}h_3(Y_{11} - h_3\theta_{11} - Y - L\psi - h_1\theta)$$

$$-2C_{2y}h_5(\dot{Y}_{11} - h_5\dot{\theta}_{11} - \dot{Y} - L\dot{\psi} - h_2\dot{\theta}) + 2K_{2\theta}(\theta_{11} - \theta) + 2C_{2\theta}(\dot{\theta}_{11} - \dot{\theta})$$

$$-2K_{1y}h_4(Y_{m1} - Y_{m2} - 2Y_{11} - 2h_4\theta_{11}) - 2C_{1y}h_4(\dot{Y}_{m1} + \dot{Y}_{m2} - 2\dot{Y}_{11} - 2h_4\dot{\theta}_{11})$$

$$-F_1b_3 = 0 \tag{3.5}$$

$$J_{1\theta}\ddot{\theta}_{12} - 4K_{1\theta}\theta_{12} + 4C_{1\theta}\dot{\theta}_{12} - 2K_{2y}h_3(Y_{12} - h_3\theta_{12} - Y - L\psi - h_1\theta)$$

$$-2C_{2y}h_5(\dot{Y}_{12} - h_5\dot{\theta}_{12} - \dot{Y} - L\dot{\psi} - h_2\dot{\theta}) + 2K_{2\theta}(\theta_{12} - \theta) + 2C_{2\theta}(\dot{\theta}_{12} - \dot{\theta})$$

$$-2K_{1y}h_4(Y_{m3} - Y_{m4} - 2Y_{12} - 2h_4\theta_{12}) - 2C_{1y}h_4(\dot{Y}_{m3} + \dot{Y}_{m4} - 2\dot{Y}_{12} - 2h_4\dot{\theta}_{12})$$

$$-F_2b_3 = 0 \tag{3.6}$$
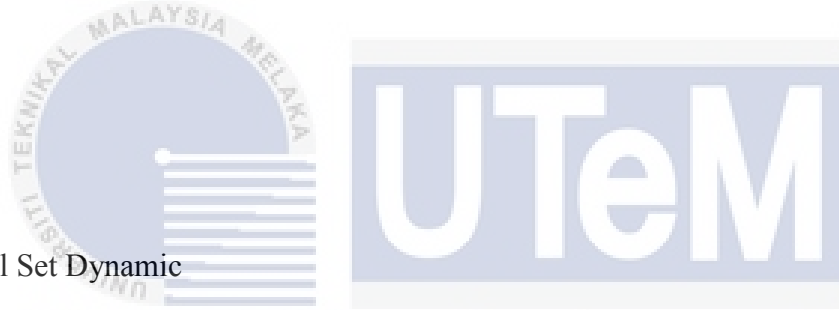
3.3.2 Wheel Set Dynamic

Equation of motion for each wheel set in lateral direction:

$$m_0\ddot{Y}_{m1} + 2K_{1y}(Y_{m1} - Y_{11} - L_1\psi_{11} - h_4\theta_{11}) + 2C_{1y}(\dot{Y}_{m1} - \dot{Y}_{11} - L_1\dot{\psi}_{11} - h_4\dot{\theta}_{11})$$

$$+2f_{22}\left(\frac{\dot{Y}_{m1}}{v} - \psi_{m1}\right) + K_gY_{m1} = 2\left(\frac{f_{22}}{v}\right)\dot{\xi}_1 + K_g\xi_1 + W\rho_1 \tag{3.7}$$

$$m_0\ddot{Y}_{m2} + 2K_{1y}(Y_{m2} - Y_{11} - L_1\psi_{11} - h_4\theta_{11}) + 2C_{1y}(\dot{Y}_{m2} - \dot{Y}_{11} - L_1\dot{\psi}_{11} - h_4\dot{\theta}_{11})$$

$$+2f_{22}\left(\frac{\dot{Y}_{m2}}{v} - \psi_{m2}\right) + K_gY_{m2} = 2\left(\frac{f_{22}}{v}\right)\dot{\xi}_2 + K_g\xi_2 + W\rho_2 \tag{3.8}$$

$$m_0\ddot{Y}_{m3} + 2K_{1y}(Y_{m3} - Y_{12} - L_1\psi_{12} - h_4\theta_{12}) + 2C_{1y}(\dot{Y}_{m3} - \dot{Y}_{12} - L_1\dot{\psi}_{12} - h_4\dot{\theta}_{12})$$

$$+2f_{22}\left(\frac{\dot{Y}_{m3}}{v} - \psi_{m3}\right) + K_gY_{n3} = 2\left(\frac{f_{22}}{v}\right)\dot{\xi}_3 + K_g\xi_3 + W\rho_3 \tag{3.9}$$

$$m_0 \ddot{Y}_{m4} + 2K_{1y}(Y_{m4} - Y_{12} - L_1\psi_{12} - h_4\theta_{12}) + 2C_{1y}(\dot{Y}_{m4} - \dot{Y}_{12} - L_1\dot{\psi}_{12} - h_4\dot{\theta}_{12})$$

$$+2f_{22}\left(\frac{\dot{Y}_{m4}}{v} - \psi_{m4}\right) + K_g Y_{m4} = 2\left(\frac{f_{22}}{v}\right)\dot{\xi}_4 + K_g\xi_4 + W\rho_4 \tag{3.10}$$

Equation of motion for each wheel set in yaw direction:

$$J_{m\psi}\ddot{\psi}_{m1} + 2k_{1\psi}(\psi_{m1} - \psi_{11}) + 2C_{1\psi}(\dot{\psi}_{m1} - \dot{\psi}_{11}) + 2f_{11}\left[\left(\frac{b\lambda}{r_0}\right)Y_{m1} + \left(\frac{b^2}{v}\right)\dot{\psi}_{m1}\right]$$

$$+C_g\psi_{m1} = 2f_{11}\left(\frac{b^2}{v}\right)\dot{\xi}_1 + C_g\xi_1 + 2\left(\frac{f_{11}\lambda b}{r_0}\right)\xi_1 \tag{3.11}$$

$$J_{m\psi}\ddot{\psi}_{m2} + 2k_{1\psi}(\psi_{m2} - \psi_{11}) + 2C_{1\psi}(\dot{\psi}_{m2} - \dot{\psi}_{11}) + 2f_{11}\left[\left(\frac{b\lambda}{r_0}\right)Y_{m2} + \left(\frac{b^2}{v}\right)\dot{\psi}_{m2}\right]$$

$$+C_g\psi_{m2} = 2f_{11}\left(\frac{b^2}{v}\right)\dot{\xi}_2 + C_g\xi_2 + 2\left(\frac{f_{11}\lambda b}{r_0}\right)\xi_2 \tag{3.12}$$

$$J_{m\psi}\ddot{\psi}_{m3} + 2k_{1\psi}(\psi_{m3} - \psi_{12}) + 2C_{1\psi}(\dot{\psi}_{m3} - \dot{\psi}_{12}) + 2f_{11}\left[\left(\frac{b\lambda}{r_0}\right)Y_{m3} + \left(\frac{b^2}{v}\right)\dot{\psi}_{m3}\right]$$

$$+C_g\psi_{m3} = 2f_{11}\left(\frac{b^2}{v}\right)\dot{\xi}_3 + C_g\xi_3 + 2\left(\frac{f_1\lambda b}{r_0}\right)\xi_3 \tag{3.13}$$

$$J_{m\psi}\ddot{\psi}_{m4} + 2k_{1\psi}(\psi_{m4} - \psi_{12}) + 2C_{1\psi}(\dot{\psi}_{m4} - \dot{\psi}_{12}) + 2f_{11}\left[\left(\frac{b\lambda}{r_0}\right)Y_{m4} + \left(\frac{b^2}{v}\right)\dot{\psi}_{m4}\right]$$

$$+C_g\psi_{m4} = 2f_{11}\left(\frac{b^2}{v}\right)\dot{\xi}_4 + C_g\xi_4 + 2\left(\frac{f_{11}\lambda b}{r_0}\right)\xi_4 \tag{3.14}$$

3.3.3 Vehicle Body Dynamic

$$M\ddot{Y} - 2K_{2y}(Y_{11} + Y_{12} - h_3\theta_{11} - h_3\theta_{12} - 2Y - 2h_1\theta)$$
$$-2\,C_{2y}\big(\dot{Y}_{11} + \dot{Y}_{12} - h_5\dot{\theta}_{11} - h_5\dot{\theta}_{12} - 2\dot{Y} - 2h_2\dot{\theta}\big) + F_1 + F_2 = 0 \tag{3.15}$$

$$J_\psi\dot{\psi} - 2K_{2\psi}(\psi_{11} + \psi_{12} - 2\psi) - 2C_{2\psi}\big(\dot{\psi}_{11} + \dot{\psi}_{12} - 2\dot{\psi}\big)$$
$$-2K_{2y}L(Y_{11} - Y_{12} - 2L\psi) - 2C_{2y}L\big(\dot{Y}_{11} - \dot{Y}_{12} - 2L\dot{\psi}\big) + (F_1 + F_2)b_4 = 0 \tag{3.16}$$

$$J_\theta\ddot{\theta} - 2K_{2\theta}(\theta_{11} + \theta_{12} - 2\theta) - 2C_{2\theta}\big(\dot{\theta}_{11} + \dot{\theta}_{12} - 2\dot{\theta}\big)$$
$$-2k_{2y}h_1(Y_{11} + Y_{12} - h_3\theta_{11} - h_3\theta_{12} - 2Y - 2h_1\theta)$$
$$-2C_{2y}h_2\big(\dot{Y}_{11} + \dot{Y}_{12} - h_5\dot{\theta}_{11} - h_5\dot{\theta}_{12} - 2\dot{Y} - 2h_2\dot{\theta}\big) + (F_1 + F_2)b_3 = 0 \tag{3.17}$$

3.4   MATLAB Simulink

The simulation of the MATLAB software 'Simulink' will be used to design the full - scale mathematical model of the railway vehicle. The mathematical model equation is represented in a block diagram using the MATLAB Simulink block library function. Modeling must follow the required equation precisely in order to avoid error during simulation execution.
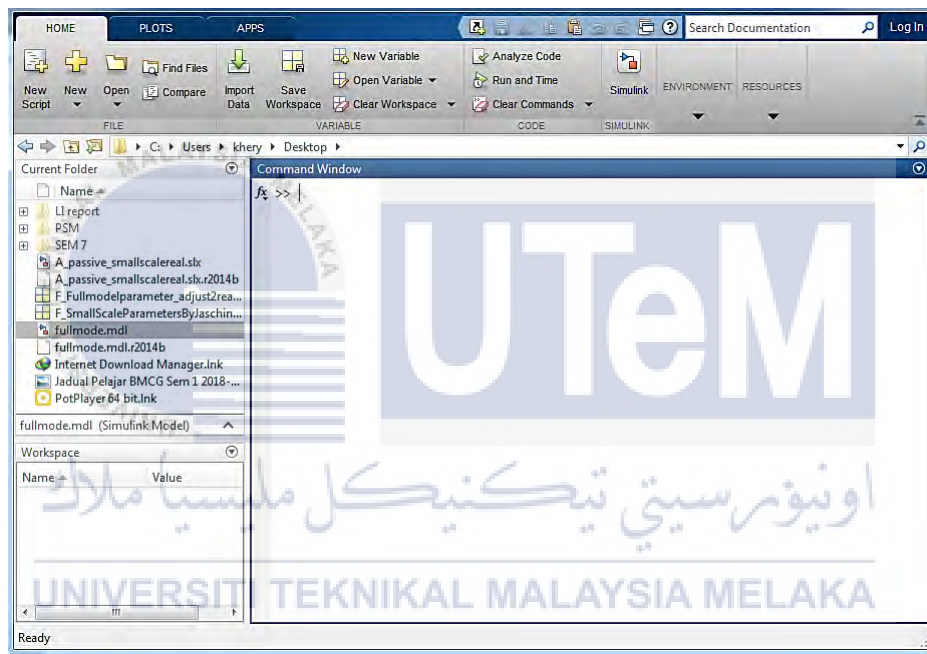

Figure 3. 3: MATLAB interface

The equation then is transferred into MATLAB SIMULINK. The frequent used function block is shown in the table below. The first step of all is to create subsystem to identify all the involved mode of motion for the body dynamic, wheel set dynamic and vehicle body dynamic. Then, to analyze the rigid body behavior, the generated acting forces is been summed.

Table 3 : Function block

Function block	Description
subsystem	To categorized the similar operation block within same area
Add	Summation of input, minus operation can be carried when negative sign is inserted
Gain	Multiplication of input, division, can be carried out when reciprocal sign is inserted.
From	Input provider, taking sources from Go to block
Go to	Sources provider for From block
Input	Create input port for subsystem
Output	Create output for subsystem
Scope	To show the graph behavior
To workspace	Graph generation
Constant	Generate constant value
Sine wave	Generate sine wave using Simulink time as time source
Step	Generate step function
Clock	Display and provide simulation time

3.5   Railway Vehicle Modelling

3.5.1   Real-scale of railway vehicle modelling

In this study, mathematical modelling starts with developing the 17-DOF full railway vehicle. The 17-DOF full railway vehicle model were represent 17 equation. It is consisting of 4 equation of lateral motion, 4 equation of yaw motion, lateral, yaw and roll motion of bogies and also lateral, yaw and roll motion of vehicle body.
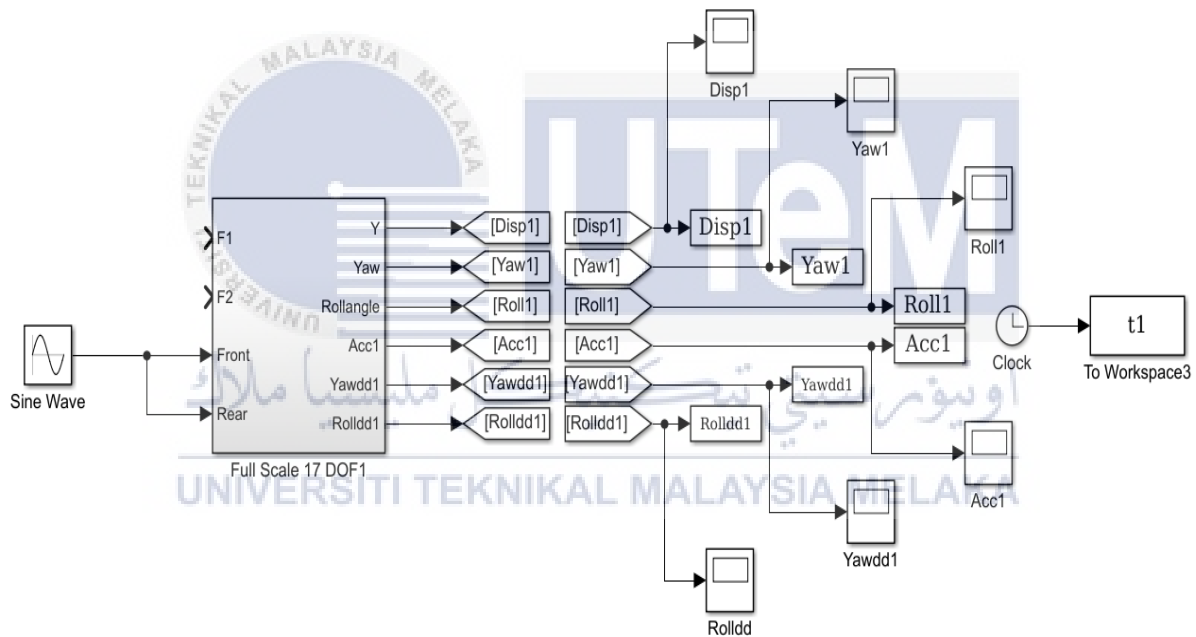

Figure 3. 4: Complete set of Simulink of Full-scale railway vehicle

Figure 3.4 show complete set of Simulink of Full-scale railway vehicle including the block subsystem of the 17-DOF in figure 3.5. Figure 3.4 also will show the simulation result of displacement, acceleration, yaw and roll against time for the full-scale model of railway vehicle. The equation of 17-DOF were insert to the block parameter (fcn) for each part of railway

vehicle. For the full-scale model, the simulation was used for three input of amplitude that is 0.07, 0.05 and also 0.01.
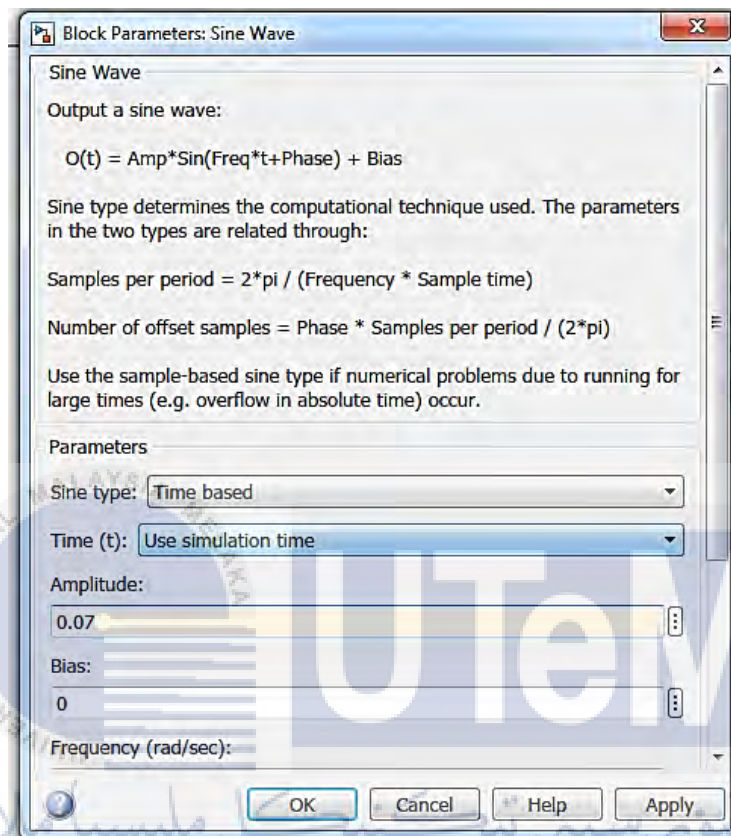

Figure 3. 5: Block parameter showing the input

3.5.2 Small-scale of railway vehicle modelling

The 17 equation of 17-DOF were same for all the method using for scaling but different parameter. The figure below shows the complete set Simulink small-scale of the railway vehicle for each scaling strategy used.
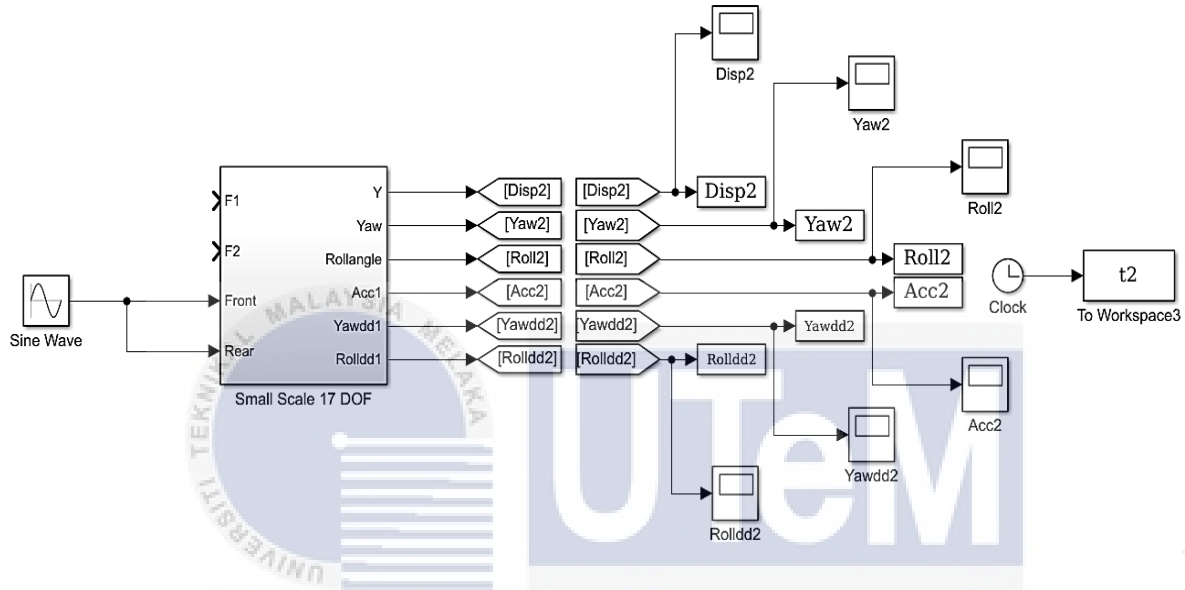

Figure 3. 6: Complete set of Simulink of small-scale for Jaschinski method railway vehicle
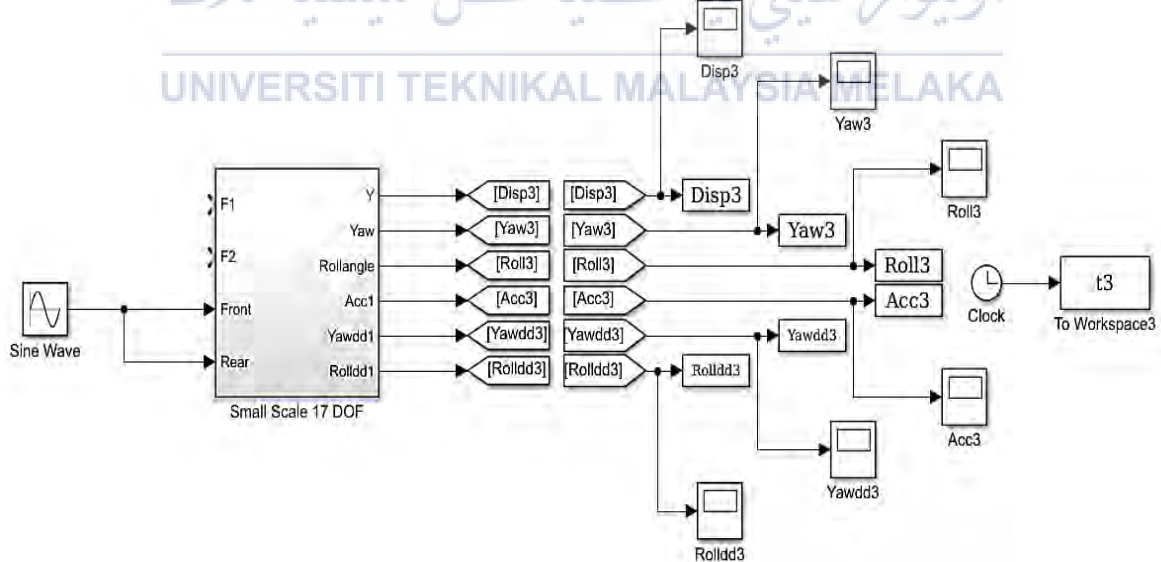

Figure 3. 7: Complete set of Simulink of small-scale for Pascal method railway vehicle
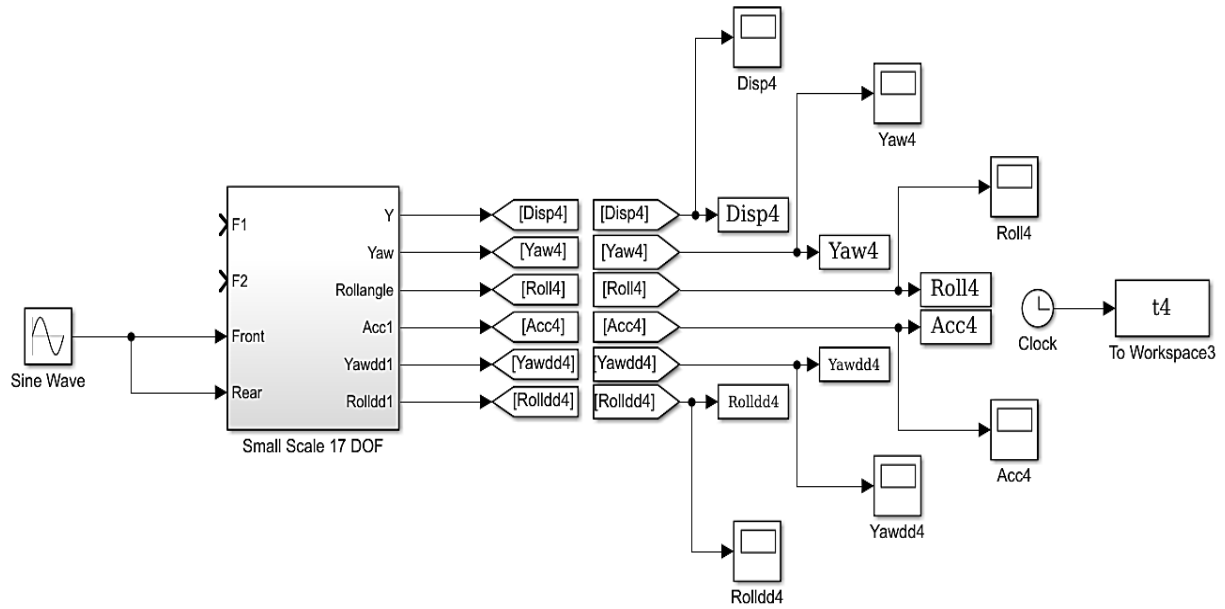
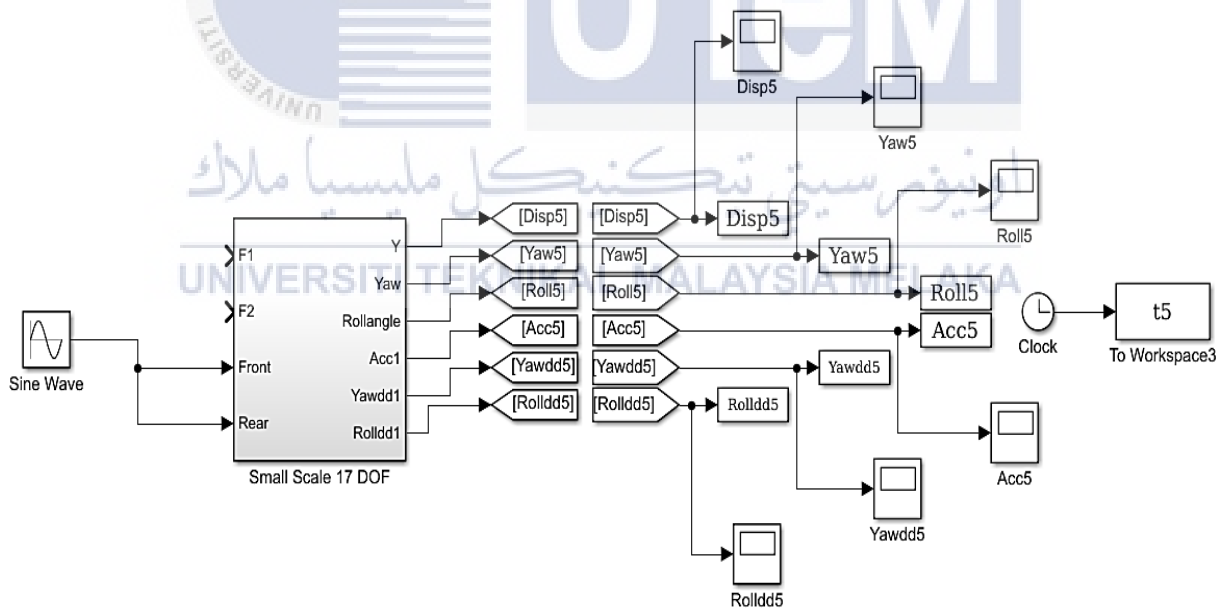Figure 3. 8: Complete set of Simulink of small-scale for Iwnicki method railway vehicle

Figure 3. 9: Complete set of Simulink of small-scale for Jaschinski modified method railway vehicle

The figure 3.5 to figure 3.8 show the complete set of Simulink of each scaling method used. The equation used and also the equation inside the Simulink is as same for all scaling method but in different parameter. The simulation for all small-scale parameter were used for three input of amplitude that is 0.014, 0.01 and also 0.002. The input was also divided by the length of each scaling strategy to make sure the simulation is same as real scaling model. From the simulation, the displacement, acceleration, yaw and roll for each method can be simulated.

3.6   Parameter Identification

The parameter used for this project were identified using the scaling factor that were introduced by Politecnico (2000) that described for each scaling method used. Table 4 below represent the parameter that were used in this project for each scaling method.

Table 4: Parameter identification for each method

Symbol	Definition	Full scale	Jaschinski	Pascal	Iwnicki	Jaschinski Modified
DOF	Degrees of freedom	17	17	17	17	17
m_c	Mass of vehicle body (kg)	32,000	256	256	256	426.67
m_{b1-b2}	Mass of bogies (kg)	3,200	25.6	25.6	25.6	42.67
m_{w1-w4}	Mass of wheelsets (kg)	1117.9	8.94	8.94	8.94	14.90
k_{1x}	Longitudinal primary spring stiffness (N/m)	3.9×10^5	15600	78000	3120	26000
k_{1y}	Lateral primary spring stiffness (N/m)	3.9×10^5	15600	78000	3120	26000
k_{1z}	Vertical primary spring stiffness (N/m)	3.9×10^5	15600	78000	3120	26000
k_{2x}	Longitudinal secondary spring stiffness (N/m)	4.5×10^3	180	900	36	300
k_{2y}	Lateral secondary spring stiffness (N/m)	4.5×10^3	180	900	36	300

k_{2z}	Vertical secondary spring stiffness (N/m)	4.5×10^3	180	900	36	300
c_{1x}	Longitudinal primary damping coefficient (Ns/m)	2.8×10^3	50.08	112	22.4	83.48
c_{1y}	Lateral primary damping coefficient (Ns/m)	2.8×10^3	50.08	112	22.4	83.48
c_{1z}	Vertical primary damping coefficient (Ns/m)	2.8×10^3	50.08	112	22.4	83.48
c_{2x}	Longitudinal secondary damping coefficient (Ns/m)	6×10^4	1073.31	2400	480	1788.85
c_{2y}	Lateral secondary damping coefficient (Ns/m)	4.5×10^3	80.50	180	36	134.16
c_{2z}	Vertical secondary damping coefficient (Ns/m)	1.8×10^3	32.20	72	14.4	53.67
I_{cy}	Yaw moment of inertia of vehicle body (kg.m^2)	123 760	39.60	39.60	39.60	66.01
$I_{b1y,b2y}$	Yaw moment of inertia of vehicle bogies (kg.m^2)	105.2	33.66×10^{-3}	33.66×10^{-3}	33.66×10^{-3}	56.11×10^{-3}

I_{cz}	Roll moment of inertia of vehicle body (kg.m^2)	41 254	13.20	13.20	13.20	22.00
$I_{b1z,b2z}$	Roll moment of inertia of vehicle bogies (kg.m^2)	35	0.0112	0.0112	0.0112	0.0187
f_{11}	Longitudinal creep force	256.3×10^4	102520	20504	-	64075
f_{22}	Lateral creep force	221.2×10^4	88480	17696	-	55300
r_o	Wheel set radius (m)	0.43	0.086	0.086	0.086	0.086
b	Wheel set spacing (m)	1	0.2	0.2	0.2	0.2
b_1	Lateral semi-spacing of radial arm bushes (m)	1	0.2	0.2	0.2	0.2
b_3	Second vertical semi-spacing of the damper (m)	1.4	0.28	0.28	0.28	0.28
b_4	Second longitudinal semi-spacing of the damper (m)	1.4	0.28	0.28	0.28	0.28
L	Distance between the central line of the bogie and vehicle body (m)	9	1.8	1.8	1.8	1.8

L_1	Semi wheel to wheel spacing (m)	1.28	0.256	0.256	0.256	0.256
h_1	Vertical distance from vehicle body center of gravity to secondary spring (m)	0.763	0.153	0.153	0.153	0.153
h_2	Vertical distance from vehicle body center of gravity to secondary damper (m)	1.36	0.272	0.272	0.272	0.272
h_3	Height from the upper line of second spring to center line of wheelset (m)	1	0.2	0.2	0.2	0.2
h_4	Height from center of sprung mass of bogie to the centre line of wheel (m)-set	1	0.2	0.2	0.2	0.2
h_5	Vertical distance from bogie frame centre of gravity to secondary lateral damper (m)	1	0.2	0.2	0.2	0.2
I_{w1-w4y}	Yaw moment of inertia of wheelsets (kg.m^2)	608.1	0.1946	0.1946	0.1946	0.3243

3.7 Experiment

3.7.1 Experimental setup

In this section, the specification of 1/5 scaled railway vehicle and the mechanism that used for the Test Rig is introduced. The Test Rig was supply by Faculty of Mechanical Engineering (FKM) of Universiti Teknikal Malaysia Melaka (UTeM). This apparatus is located at the Machinery Building Workshop of FKM. The experiment were conducted to find out the actual data of the Test Rig and do the validation with the simulation result on the MATLAB. The Test Rig composed of wheelset, bogie, half carbody and also suspension but the experimental were only focus on the lateral motion of the carbody. The Rig were already rusty and the mechanism for the vehicle were already gone. The mechanism were designed so that the Test Rig corresponding to the rail is controlled by the motor according to its speed command.

Figure 3. 10 : The Test Rig of the railway vehicle

3.7.2 Mechanism on the test rig

For the Test Rig experimental setup, the mechanism to push the Test Rig were designed using SOLIDWORK software. A simple model of mechanism were designed to represent the real mechanism that will be fabricated and attached to the Test Rig. All the measurement that used in the SOLIDWORK were set to mm and used for the real measurement in the fabrication.
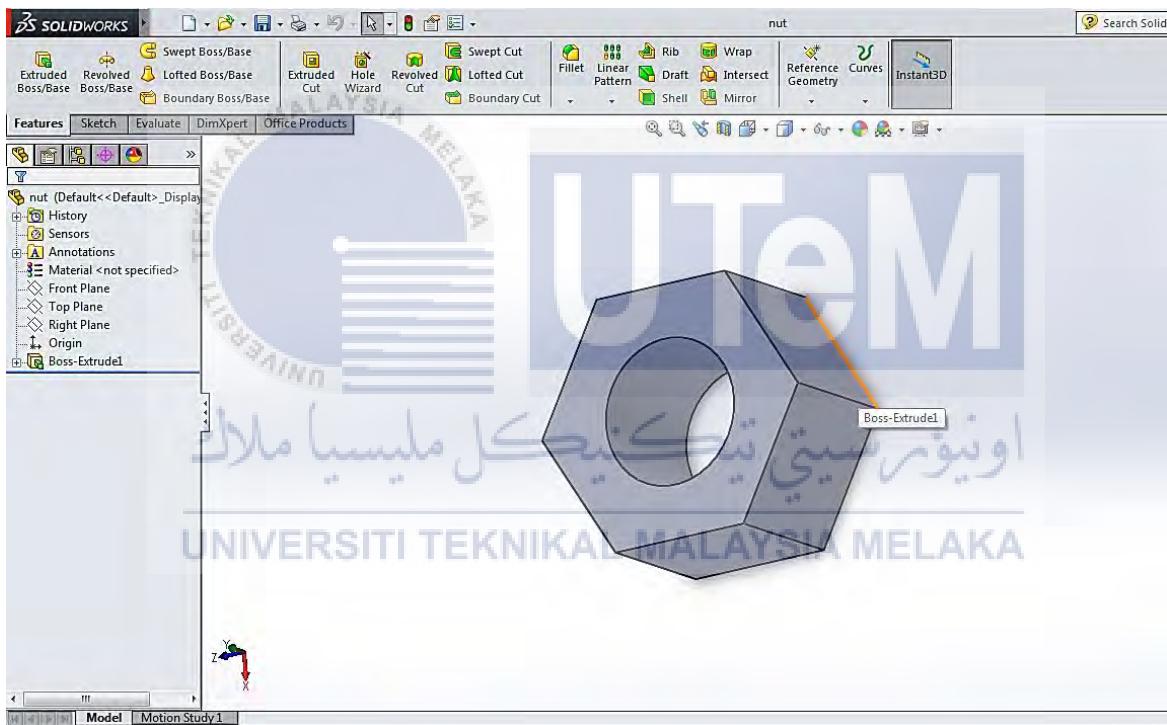

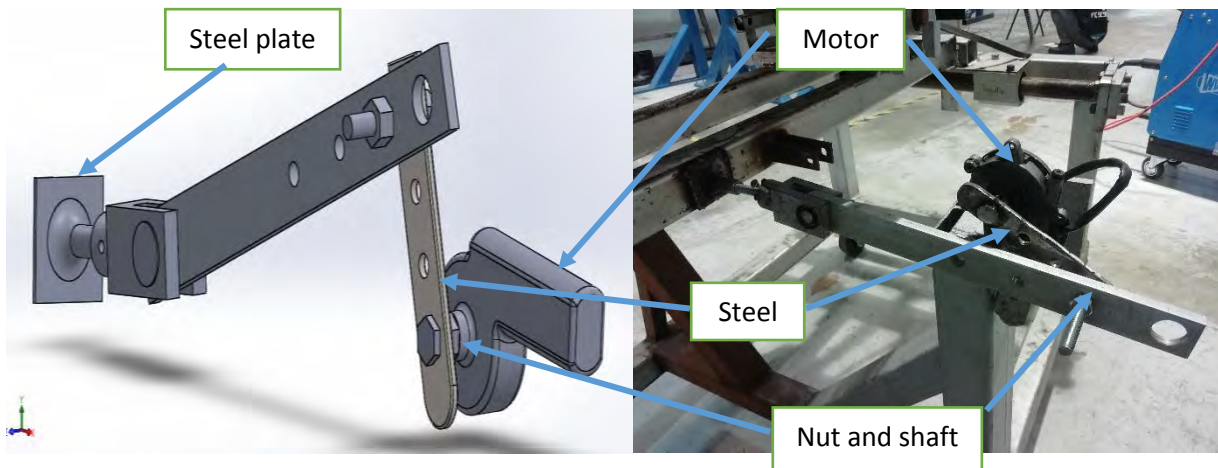Figure 3. 11 : SOLIDWORK software interface

3.7.2.1 The mechanism

Figure 3. 12 : The mechanism that used on the Test Rig

As shown in the above figure, the mechanism use a power window motor as a power to push the car body of the railway vehicle or the Test Rig. The first steel were 150mm x 30mm x 5mm in measurement. There are 4 holes with 10mm diameter and 30mm distance for each other. One hole were weld with the motor so that its hold and rotate without any difficulty. Then, other three hole will be connected with other steel that 330mm x 4mm x 5mm with a nut and attached it so the mechanism can function. The second steel were connected to the bearing. The steel plate with 50mm x 50mm were weld to the Test Rig and connected with the bearing so it can function along with the mechanism. The steel plate were connected to the shaft and then tighten with screw and nut so that the grip with the shaft more firm. The full dimension for all the drawing are provided in the appendix.
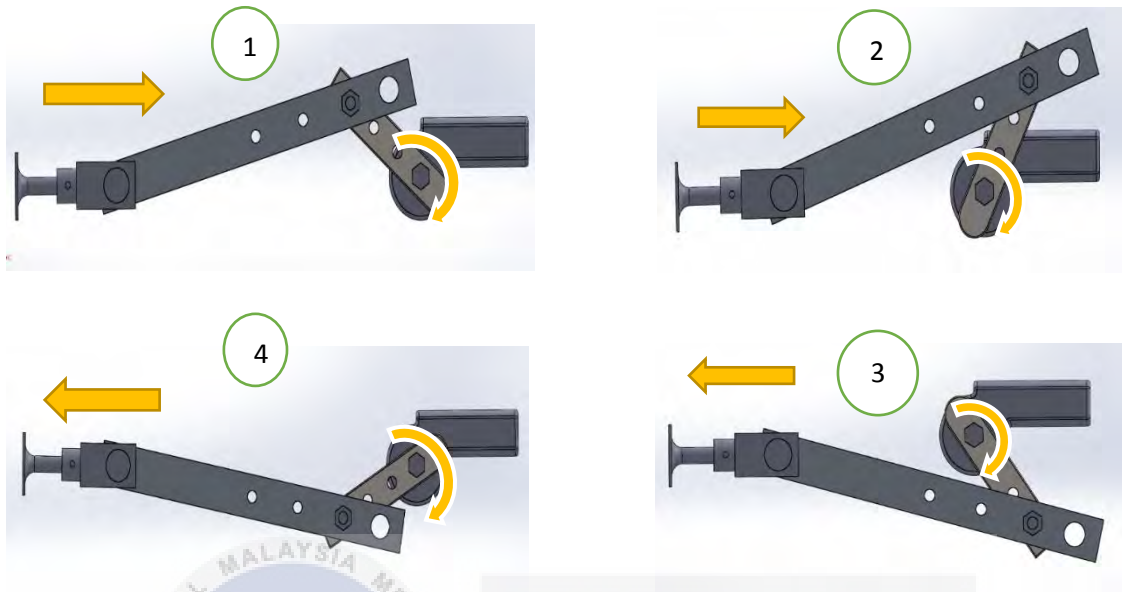
Figure 3. 13 : The movement of the mechanism

The movement of the mechanism were more to push and pull the Test Rig. Firstly the motor were connected to the 12V of battery and placed at the side of the Test Rig. The switch were provided as to switch on the motor. The motor can be turn clockwise and anticlockwise but in this experiment, the motor only will turn clockwise. As shown in the figure 3.12, the first and second figure shown how the motor turn clockwise and pull the steel that connected with it. Then, the steel plate that already weld with the Test Rig will pull it moving along with the motor. After that, as the motor turn, the mechanism will push the Test Rig as shown in third and fourth figure. As the motor turn on, the routine will be repeated and the mechanism will continue push and pull the Test Rig.

3.7.3 Sensor

There are several sensor that used for the Test Rig to measure the displacement, body angle the vehicle and also the body acceleration of the railway vehicle. The sensors were placed at the test rig and connected to the computer to measure and came out with the experimental graph.

Table 5 : Sensor

| Linear variable differential transformer (LVDT)	The LVDT is a type of electrical transformer used for measuring linear displacement (position). LVDT is used for linear displacement measurements. LVDT also record the track input of the Test Rig.
Accelerometer Sensor	Accelerometer is used for measure a vehicle acceleration. It also can be used to measure vibration on car, building and also safety installation. For Test Rig, the sensor were placed to get the actual data of the acceleration on the Test Rig.
Gyro Sensor	Gyro sensor were functioned to measure the yaw and also the roll angle of the Test Rig. The pitch angle were no discussed in the experiment as the Test Rig were assumed that pitch not involved in the experiment.
Computer Set	The three sensor will be connected to the computer as a medium to analysis the data and also the graph from the sensor.
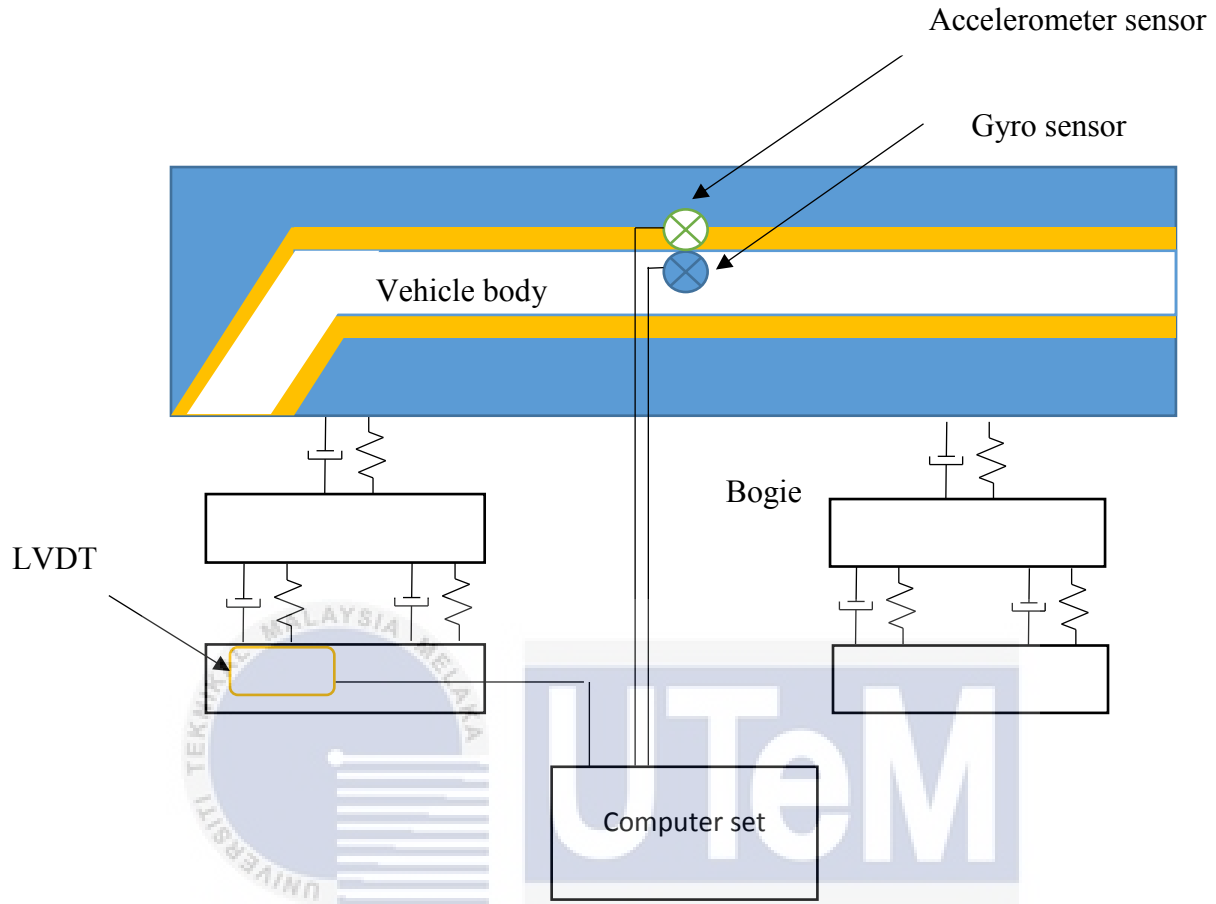
Figure 3. 14: The sensor placement at the Tet Rig

The figure above show the schematic diagram of the sensor placement at the Test Rig. The LVDT is place at the side of the Test Rig to record the track input. The input were random and will be used as the input for the experimental input and also the simulation for the validation. Then, the gyro sensor were placed at the center of the Test Rig. The angular velocity or the roll were measure by the sensor's own movement. Angle are detected via integration operation by a computer. The angle moved is fed up to and reflected in an application. So the gyro were more to measure yaw angle and roll angle of the Test Rig. After that, the accelerometer sensor were placed beside gyro sensor. The accelerometer is electromechanical device that used to measure

acceleration. Accelerometer allow user to understand the surrounding of Test Rig better. All the three sensor were connected to the computer set to get the data and also the graph that needed.

3.8 Verification of the Model

Verification of the model will be done in the simulation to find the accuracy and also the behavior of the simulation. The verification will be done by validate the simulation and also the experiment result and compare each behavior for displacement, roll and also acceleration.
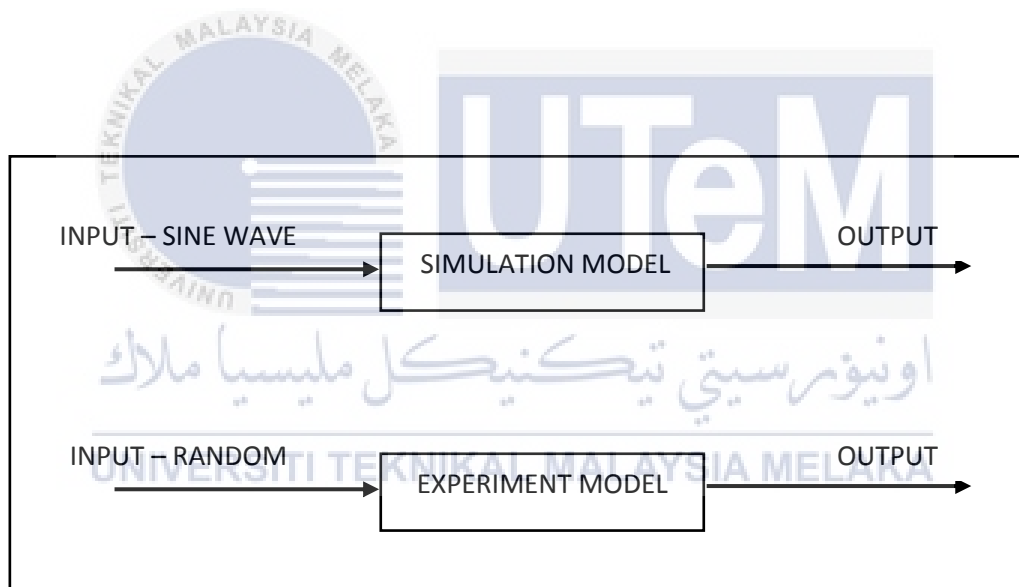
Figure 3. 15 : Schematic of system

As shown in the figure 3.14, it is a simple schematic of system that used in this project. It is the schematic before the validation model happen. For the simulation model, it based on the MATLAB SIMULINK model that use the scaling model based on the selection. The input that were used for the selection model is the sine wave input so the graph will be sinusoidal equally according to the dimensional analysis provided. For the experiment model, the input that used

were different. The input were random based on the how the experiment had been done. With the mechanism that had been fabricated, the Test Rig also had been pushed manually and that why the input were random.
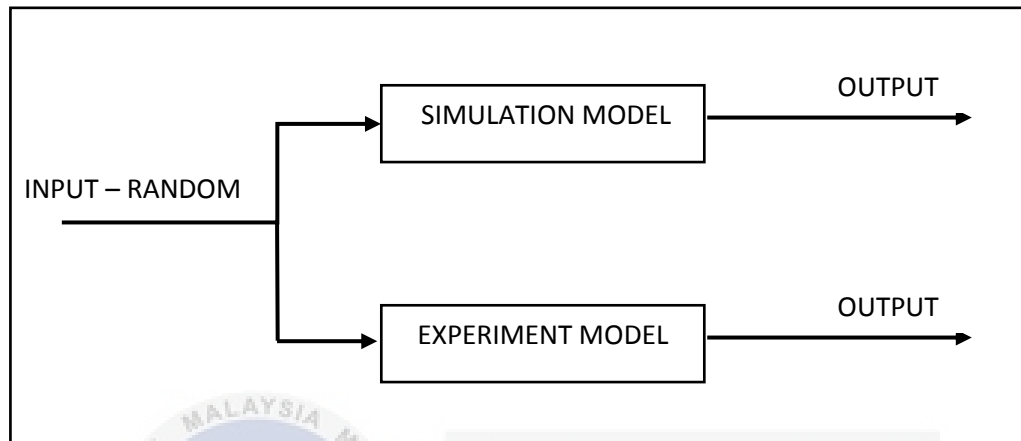

Figure 3. 16 : Schematic of the validation system

For the verification of the model, the simulation and experiment model will be validate based on the acceleration, yaw and roll angle. But the input for the validation will use only the random input because when to compare the graph it will be need an actual input for the validation for verify that model is valid. The dimensional analysis that used earlier for the simulation will be used first to see the pattern that needed for the selection model.

CHAPTER 4

RESULT AND ANALYSIS
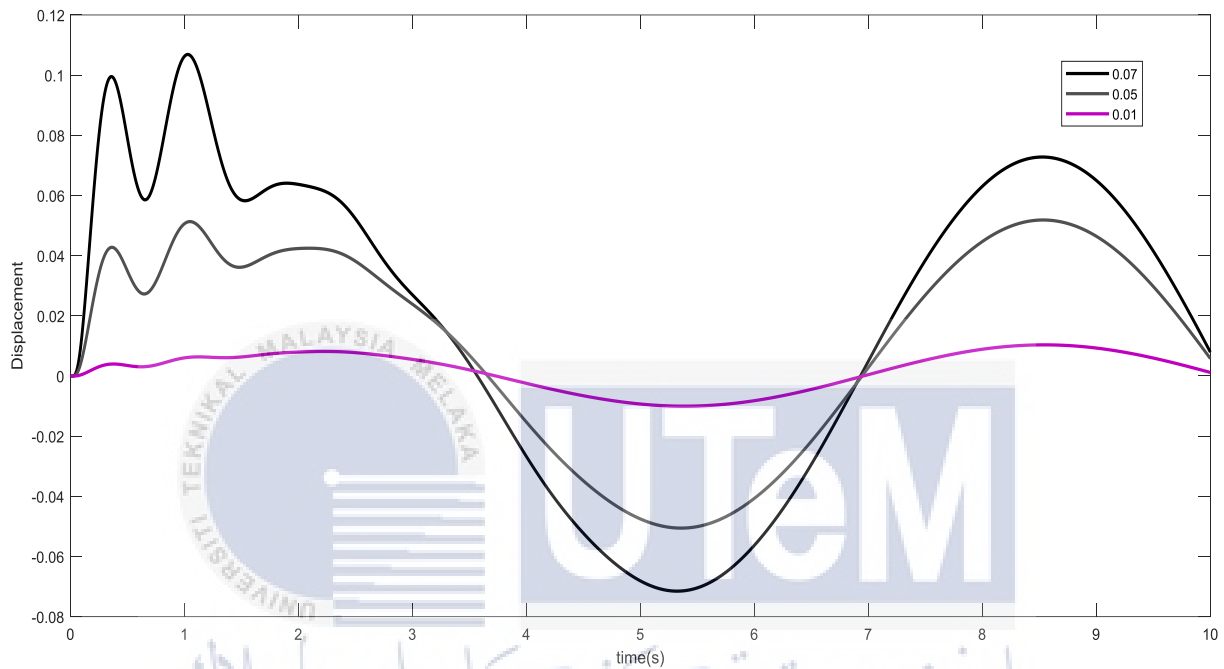
4.1   Displacement Result

Figure 4. 1: Real-scale displacement graph for 3 input

Figure 4.1 shows the real-scale of the displacement graph of the 3 input after the simulation done. The real scale used a real parameter that were put into the simulation but using three different of the amplitude inputs that is 0.07, 0.05 and 0.01. From the graph, the variety of pattern can be seen to differentiate the three input with 0.07 input reached the maximum displacement. As the smaller input were given to the simulation, the amplitude of the graph can be minimized to the minimum.
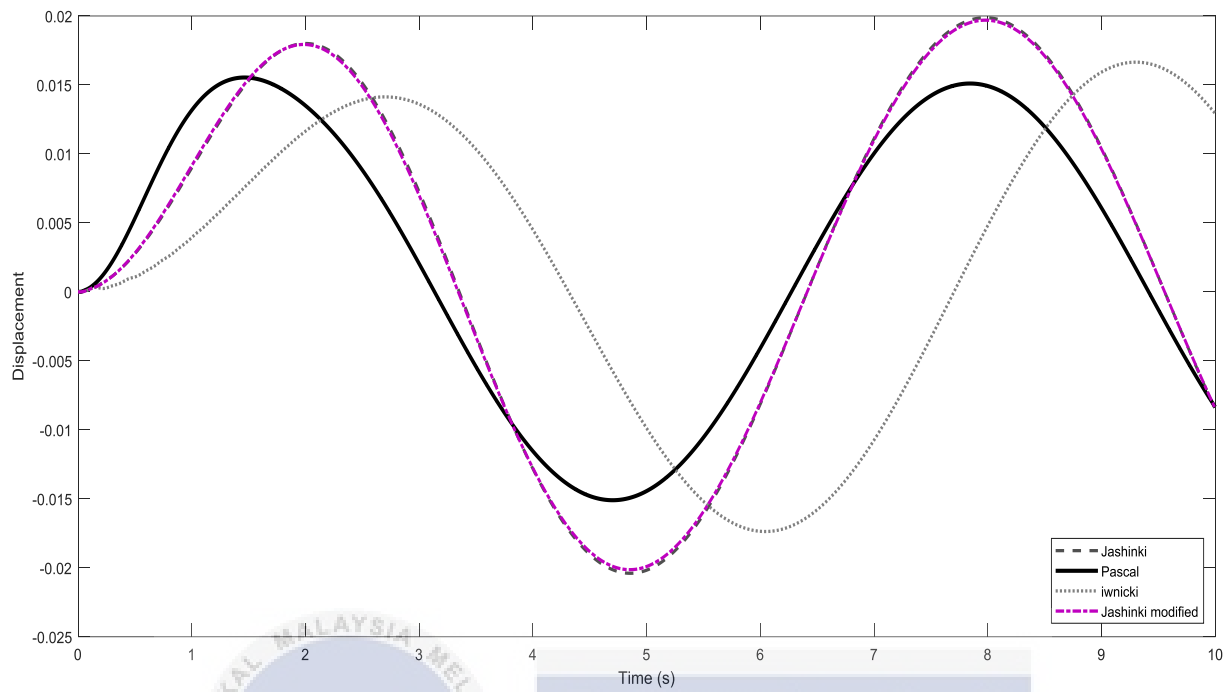
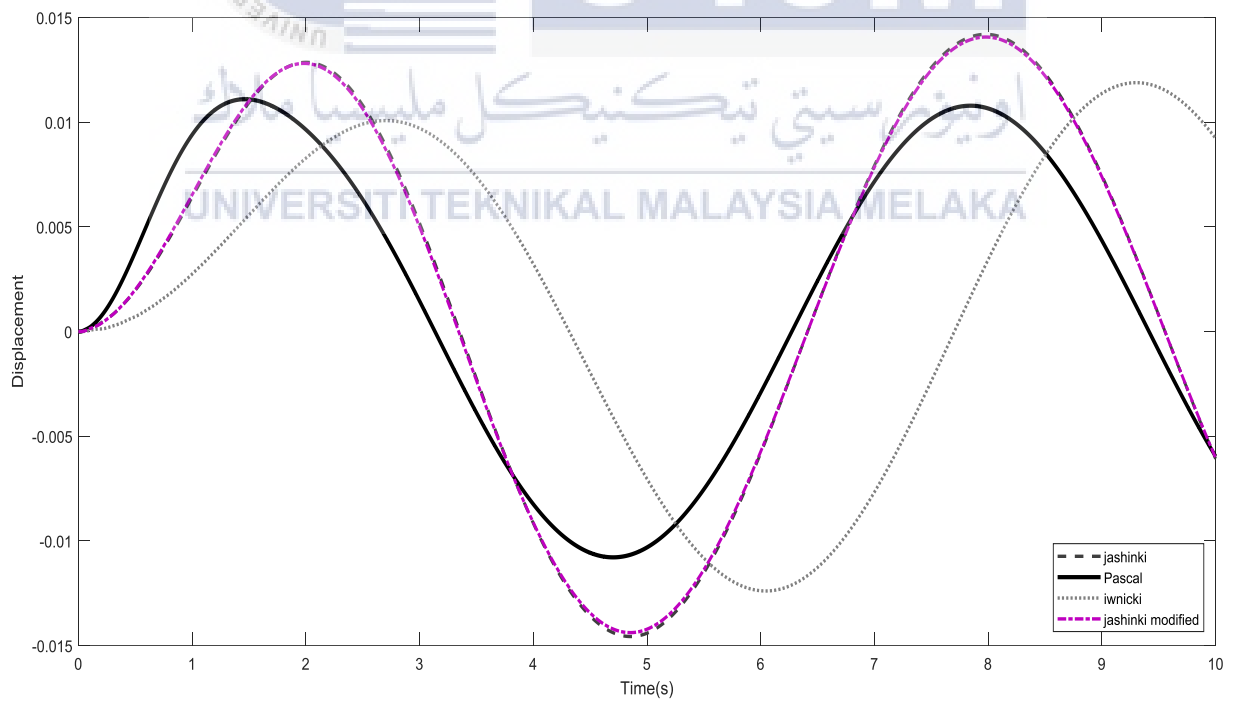Figure 4. 2: Small-scale method for input 0.014

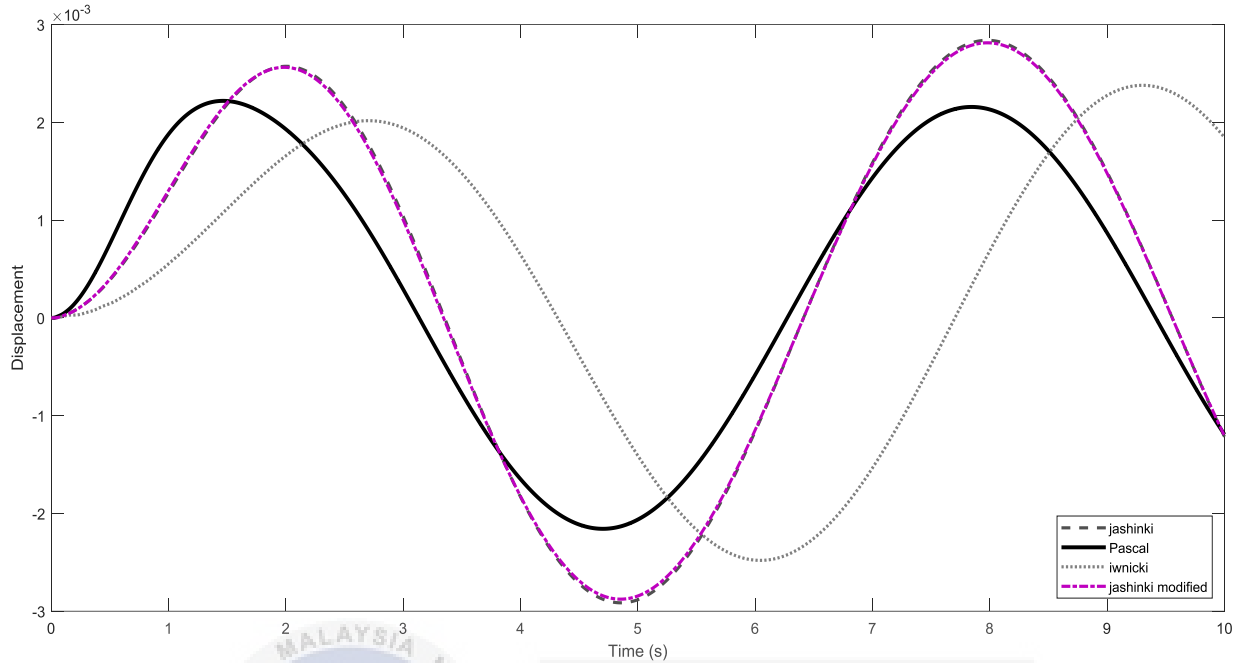Figure 4. 3: Small-scale method for input 0.01

Figure 4. 4: Small-scale method for input 0.002

Figure 4.2 to figure 4.4 show a displacement graph of the scaling method used for the input 0.014, 0.01 and 0.002. The input was divided by scale of 5 to make sure the scaling method's result will be as same as real scale. The method used such as Jaschinski, Pascal, Iwnicki and Jaschinski modified were simulated in MATLAB Simulink and the result were combined as shown in the figure 4.2 to figure 4.4 according to their input. As for the displacement criteria, the Pascal method had been chosen as the pattern of the graph as nearly to the real scale. As for the real scale, the graph starts to rise before time 1 second period and catches the maximum number at 1 second. The Pascal method is the closest pattern when the graph of the reached the maximum number. It the same pattern for the three input as the Pascal method is the most suitable for the displacement.

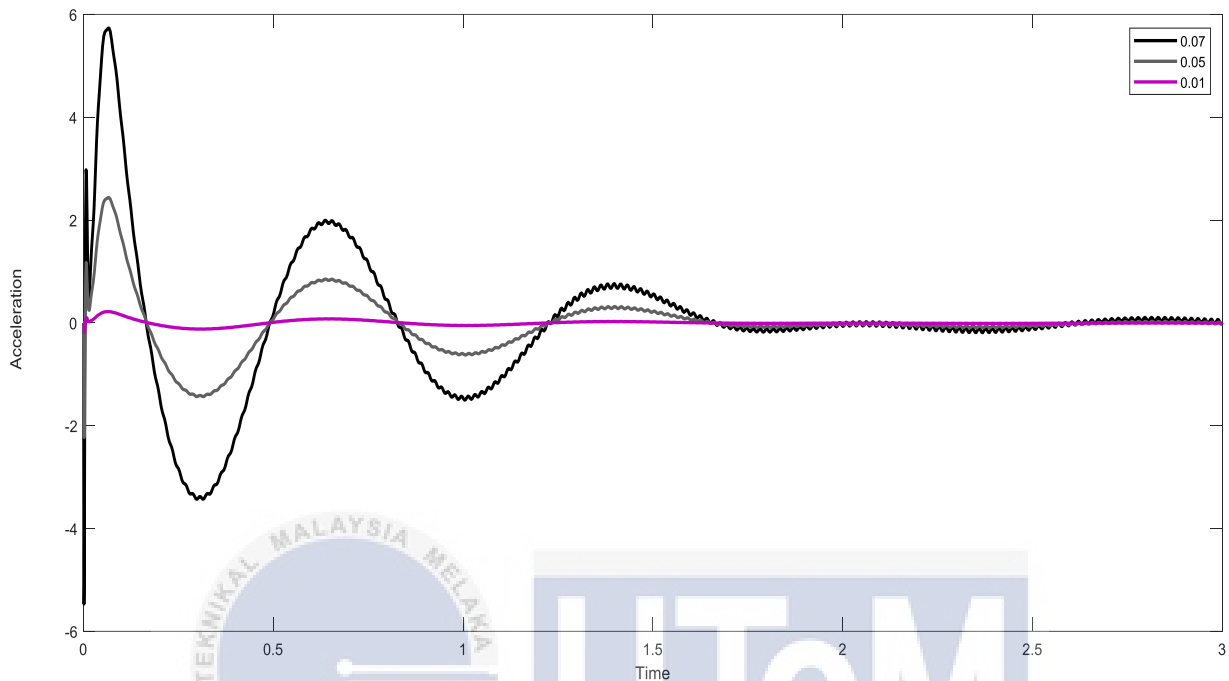**4.2   Acceleration Result**

Figure 4. 5: Real-scale acceleration graph for 3 input

Figure 4.5 shows the real-scale of the acceleration graph of the 3 input after the simulation done. The real scale used a real parameter that were put into the simulation but using three different of the amplitude inputs that is 0.07, 0.05 and 0.01. from the graph, the variety of pattern can be seen to differentiate the three input with 0.07 input reached the maximum acceleration as the smaller input were given to the simulation, the amplitude of the graph can be minimized to the minimum. The time taken were for 10 second but the starting at 3 second the pattern of the graph has started become straight line at zero for acceleration. So, for more details of the pattern, the graph only takes at 3 second for easier analysis.
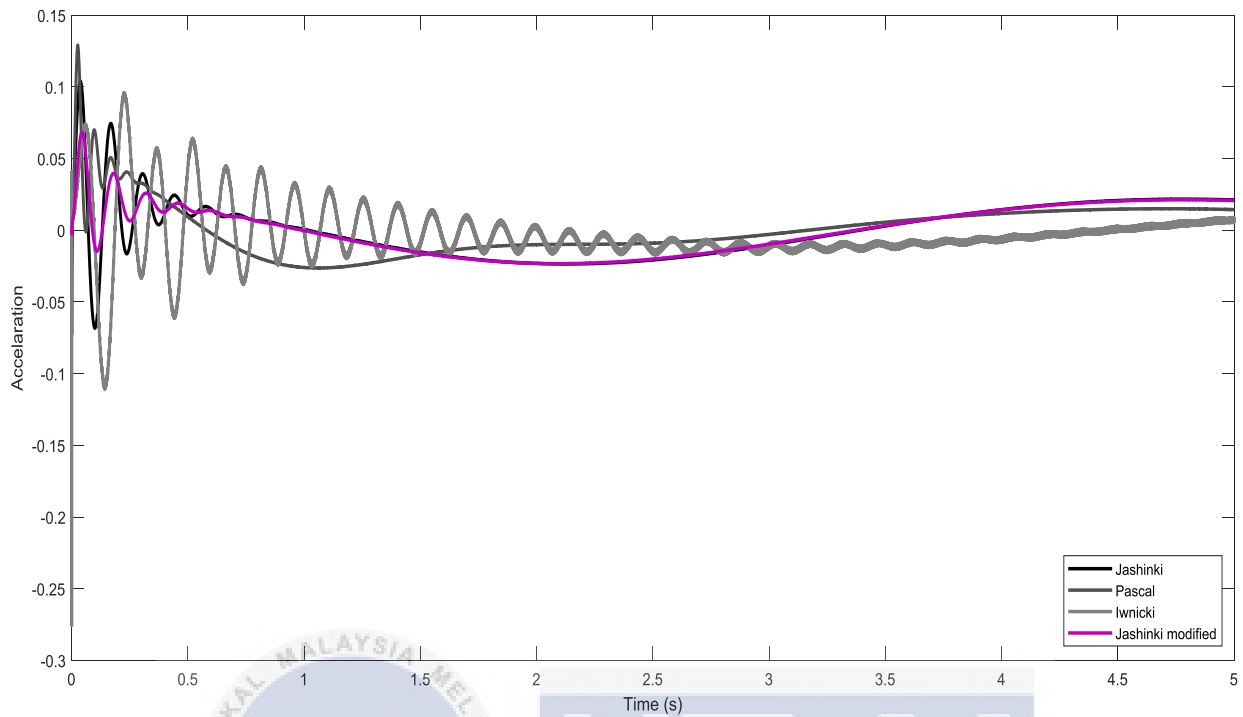
Figure 4. 6: The small-scale method for input 0.014

Figure 4.6 show the graph of small-scale method for input 0.014. For some reason, the pattern of the graph looks a bit chaotic as the different of the parameter used by different method. As the solution, the Iwnicki method had to be released because the graph become more fibrous and disturb the analysis. The graph of acceleration only used three method; Jaschinski, Pascal and also Jaschinski modified.
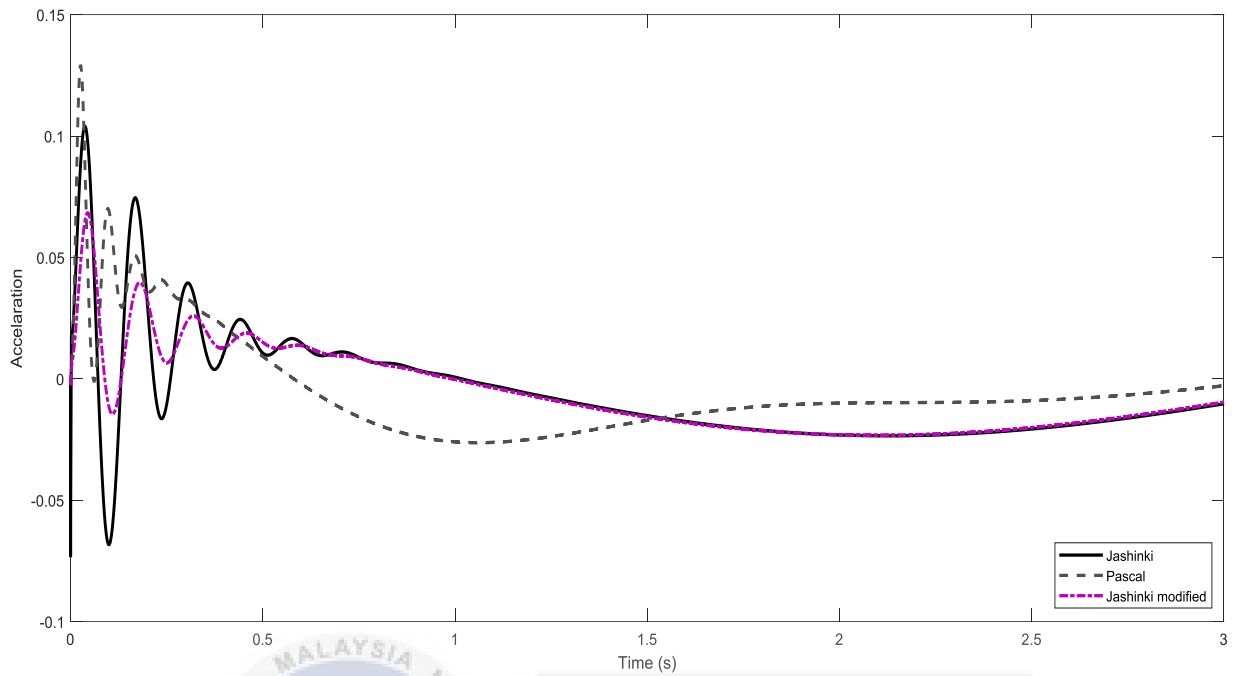
Figure 4. 7: Small-scale method for input 0.014 without Iwnicki
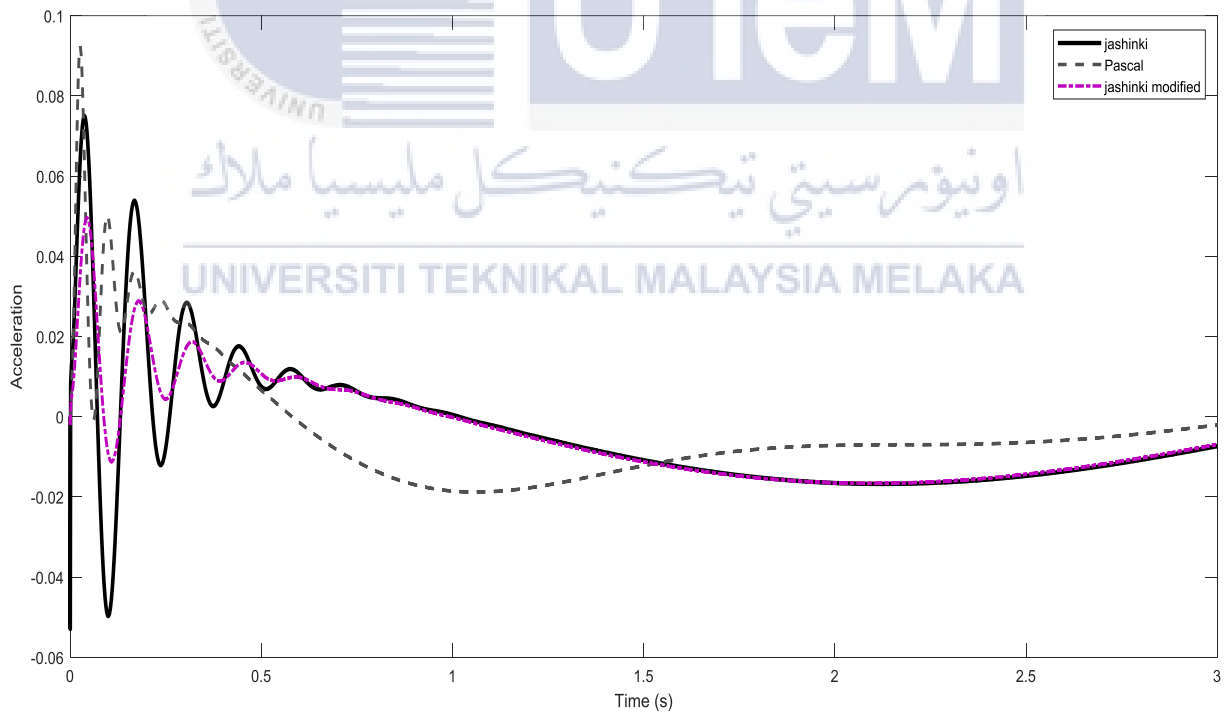

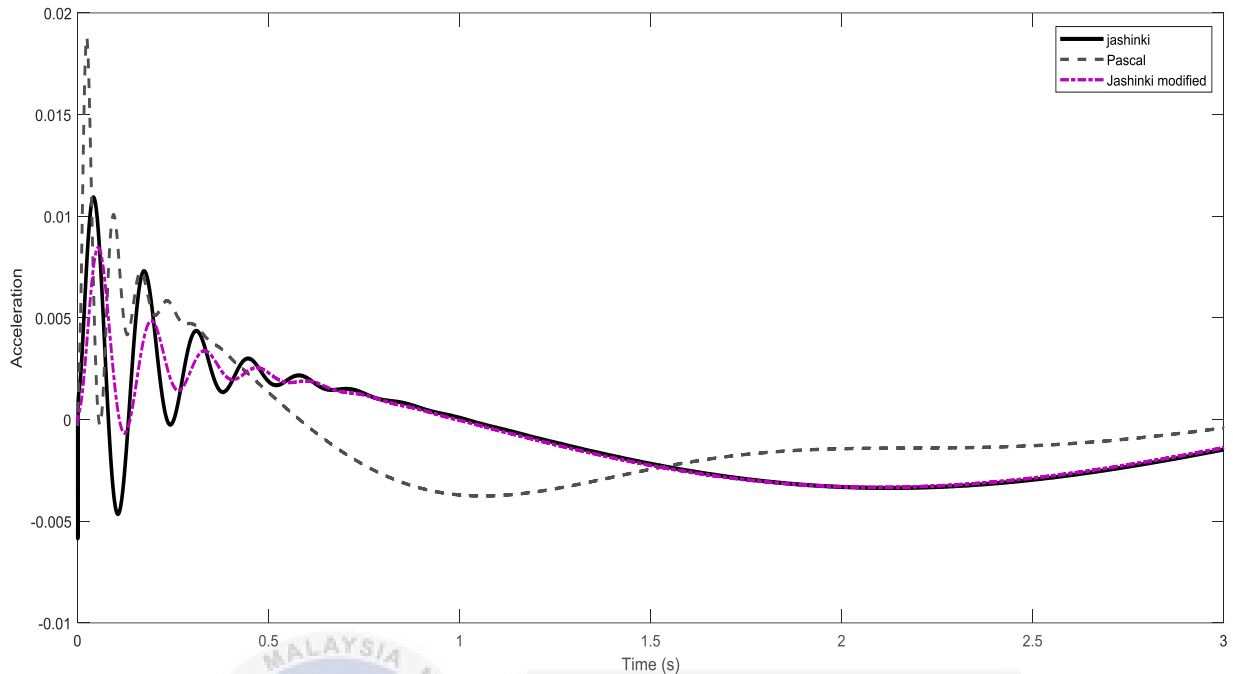Figure 4. 8: Small-scale method for input 0.01 without Iwnicki

Figure 4. 9 :small-scale method for input 0.002 without Iwnicki

Figure 4.7 to figure 4.9 shows a small-scale method involving only 3 method that is Jaschinski, Pascal and Jaschinski modified for each scaled input. From the graph, the Jaschinski were chosen as a suitable method to carry out the acceleration for each input. Jaschinski method show a likely pattern to the real scale and it is consistent for each input. As for Pascal method, the pattern of graph keeps changing. The changes can be seen through the three graphs as the lower the number of the input, the graph keep increase the maximum amplitude of the method. Alongside that, the Iwnicki and Jaschinski modified method also keep changing the pattern when the input given were different. But different with Jaschinski method as the pattern keep same although the input was change.
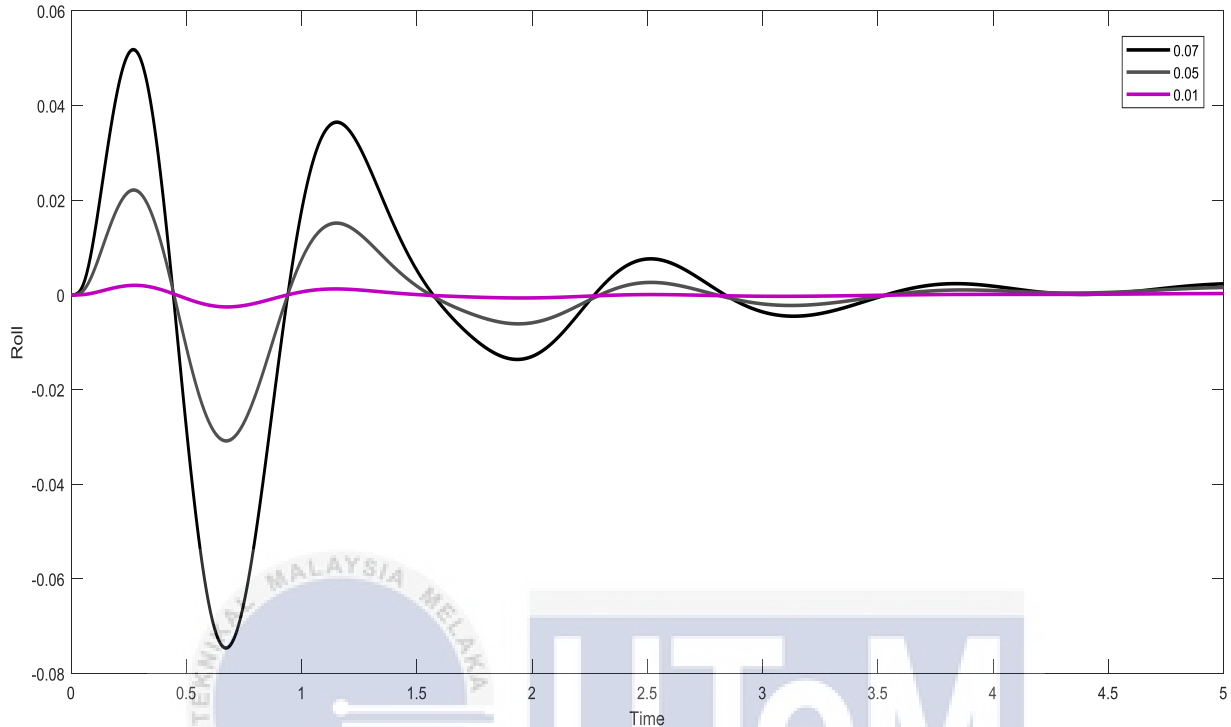
4.3   Roll Result

Figure 4. 10 : Real-scale roll graph for 3 input

Figure 4.10 shows the real-scale of the roll graph of the 3 input after the simulation done. The real scale used a real parameter that were put into the simulation but using three different of the amplitude inputs that is 0.07, 0.05 and 0.01. Roll is the x-axis for the railway vehicle analysis. From the graph, the variety of pattern can be seen to differentiate the three input with 0.07 input reached the maximum roll. As the smaller input were given to the simulation, the amplitude of the graph can be minimized to the minimum. The time taken were for 10 second but the starting at 5 second the pattern of the graph has started become straight line at zero for roll behavior. So, for more details of the pattern, the graph only takes at 5 second for easier analysis.
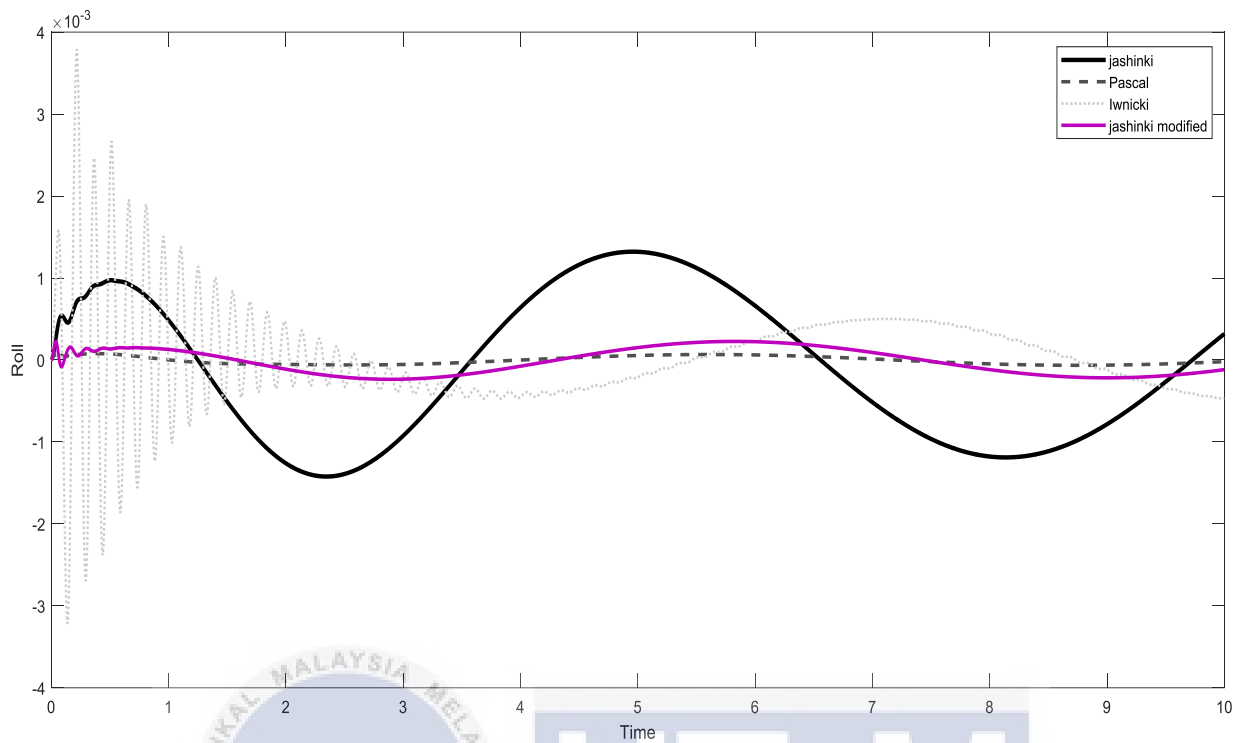
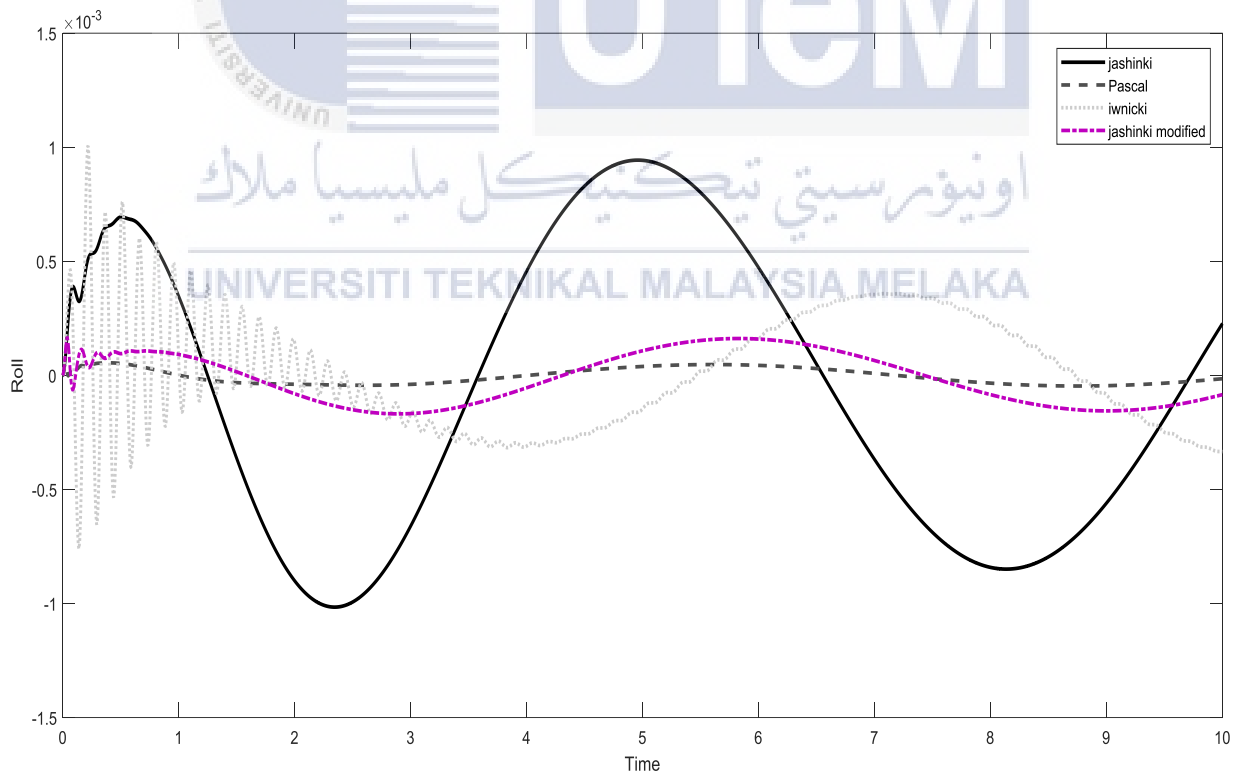Figure 4. 11 : The small-scale method for input 0.014

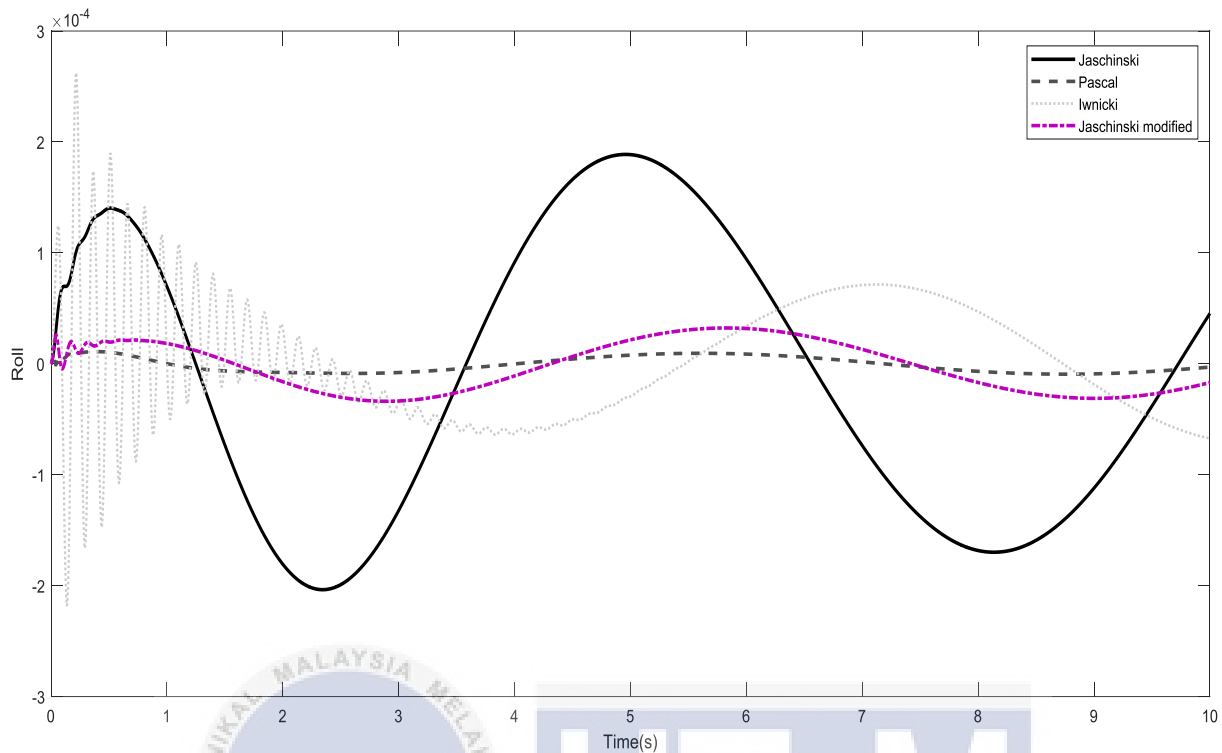Figure 4. 12 : The small-scale method for input 0.01

55

Figure 4. 13 : The small-scale method for input 0.002

The small-scale for the scaling method for roll were shown in the figure 4.11 to figure

4.13. As shown in the graph, the variety of the graph had been simulated but for the roll

criteria, three method had been chosen as the closest pattern to the real scale. For Jaschinski

method, the method can be used for real scale at input 0.07 as the graph achieved the

maximum higher than another pattern. For a input 0.01 and 0.05, the Pascal method and

Jaschinski's method can be used as the pattern of the graph likely suitable. The graph keeps

consistent nearly to the zero point as same as real scale graph and had a minimum amplitude

for all scaling method.
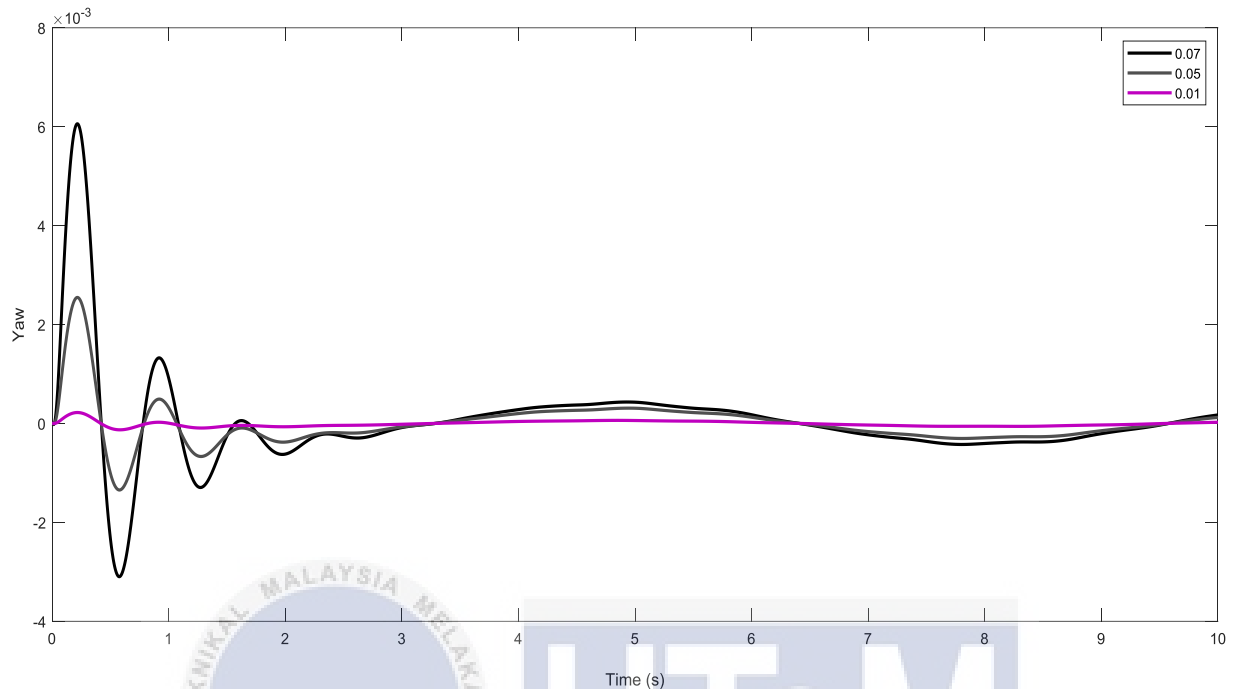
4.4   Yaw Result

Figure 4. 14 : Real-scale yaw graph for 3 input

Figure 4.14 shows the real-scale of the yaw graph of the 3 input after the simulation done. The real scale used a real parameter that were put into the simulation but using three different of the amplitude inputs that is 0.07, 0.05 and 0.01. Roll is the y-axis for the railway vehicle analysis. From the graph, the variety of pattern can be seen to differentiate the three input with 0.07 input reached the maximum yaw. As the smaller input were given to the simulation, the amplitude of the graph can be minimized to the minimum. Starting from 4 second, the yaw graph start in a straight line as the increase of the time, the fluctuation of the graph decrease.
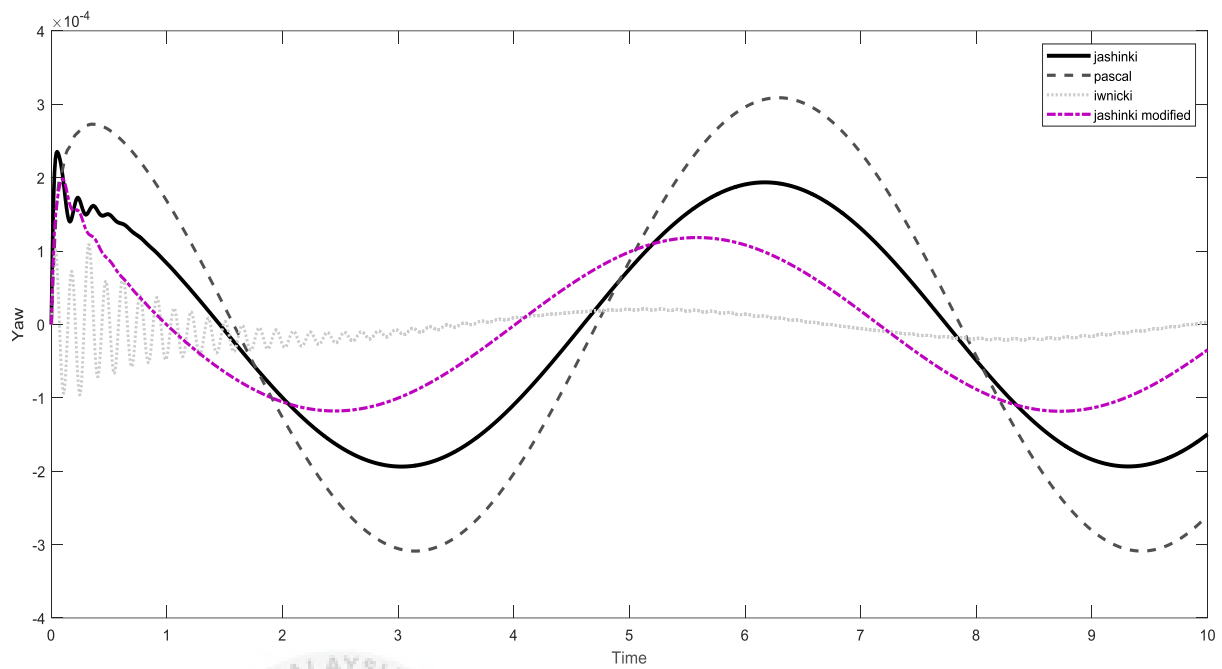
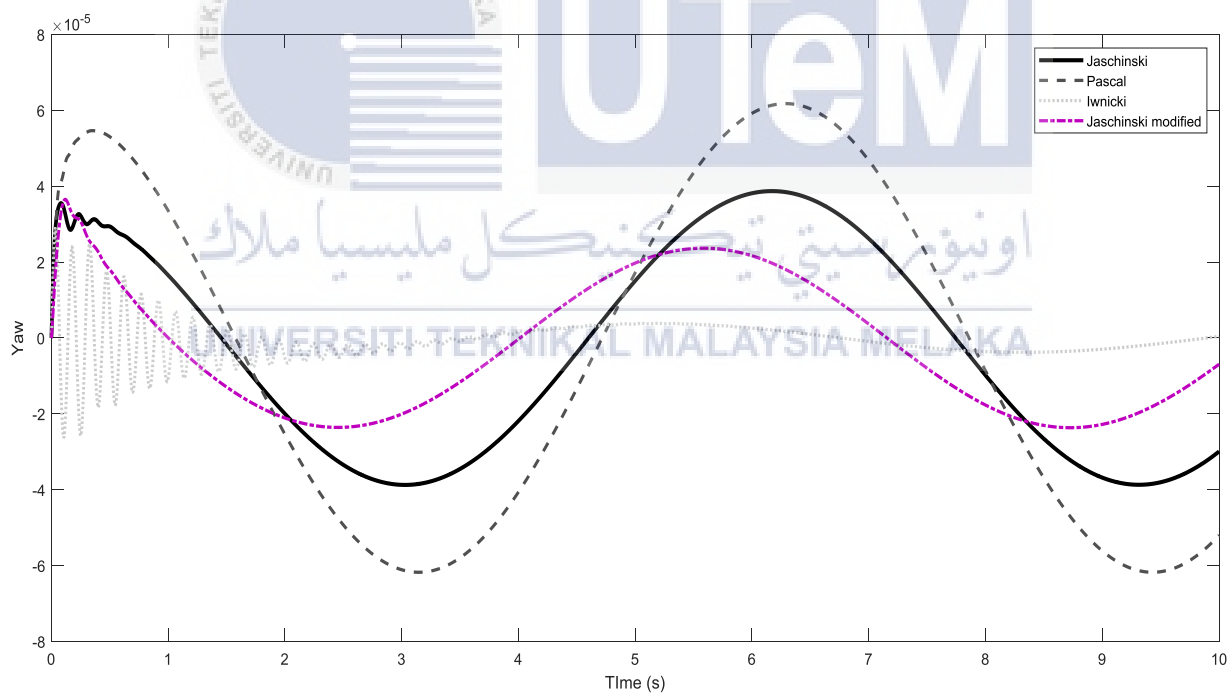Figure 4. 15 : The small-scale method for input 0.001

Figure 4. 16 : The small-scale method for input 0.002
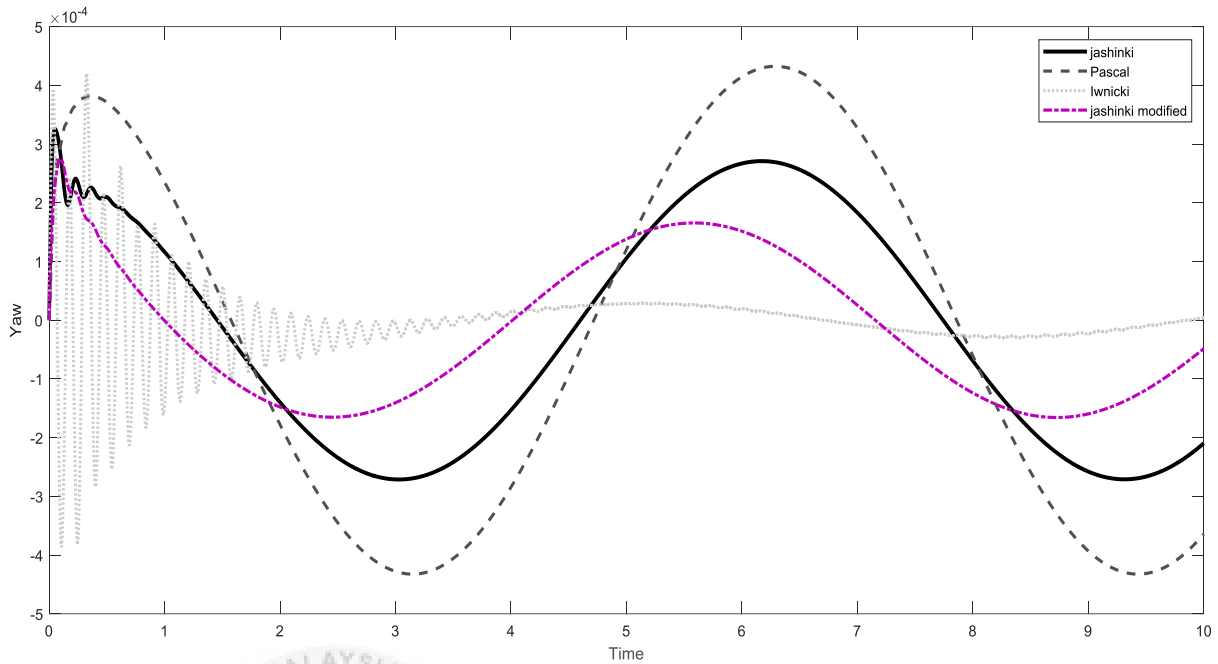
Figure 4. 17 : The small-scale method for input 0.014

The small-scale for the scaling method for roll were shown in the figure 4.15 to figure 4.17. As shown in the graph, the variety of the graph had been simulated but for the roll criteria, three method had been chosen as the closest pattern to the real scale. For Jaschinski method, the method can be used for real scale at input 0.07 as the graph achieved the maximum higher than another pattern. For an input 0.01 and 0.05, the Pascal method and Jaschinski's method can be used as the pattern of the graph likely suitable. The graph keeps consistent nearly to the zero point as same as real scale graph and had a minimum amplitude for all scaling method.

59

Table 6 : the analyzed result

	Jaschinski	Pascal	Iwnicki	Jaschinski modified
Displacement	X	O	X	X
Acceleration	O	X	X	X
Roll	O	O	X	O
Yaw	O	O	X	O

O = accepted

X = not Accepted

From the table 4, the study was concluded that not every method can be used for the certain calculation or simulation. As for the simulation of the displacement, only the pascal method can be used as the pattern of the graph were similar to the real scale pattern. Next, for the acceleration, only Jaschinski method can be used as the pattern were likely same as real scale. The Iwnicki method cannot be used as the pattern were to rarely distribute. As for the roll perspectives, three method can be used, Jaschinski, Pascal, and also Jaschinski modified as the graph shown the pattern that suitable for the real scale but for Pascal and Jaschinski Modified , it can only use for input of 0.02 and 0.05 as the graph more suitable for the an input that lower than 0.05. Same as the yaw perspectives, three method can be used. That is Jaschinski, Pascal and also Jaschinski modified.
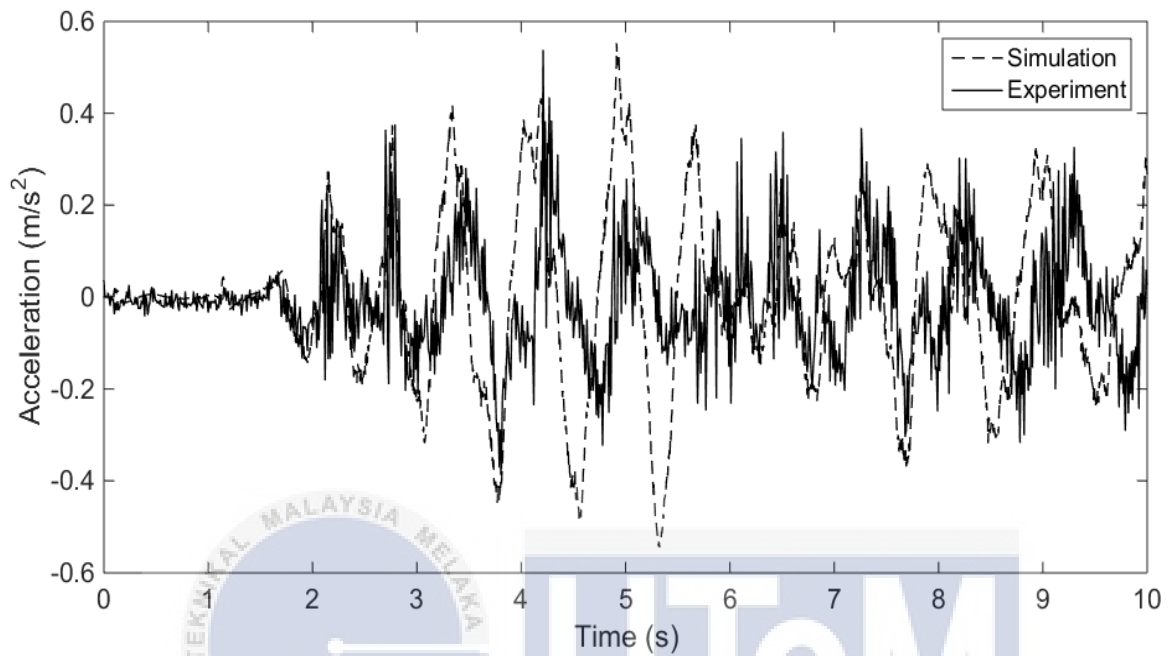
4.5 Validation Result

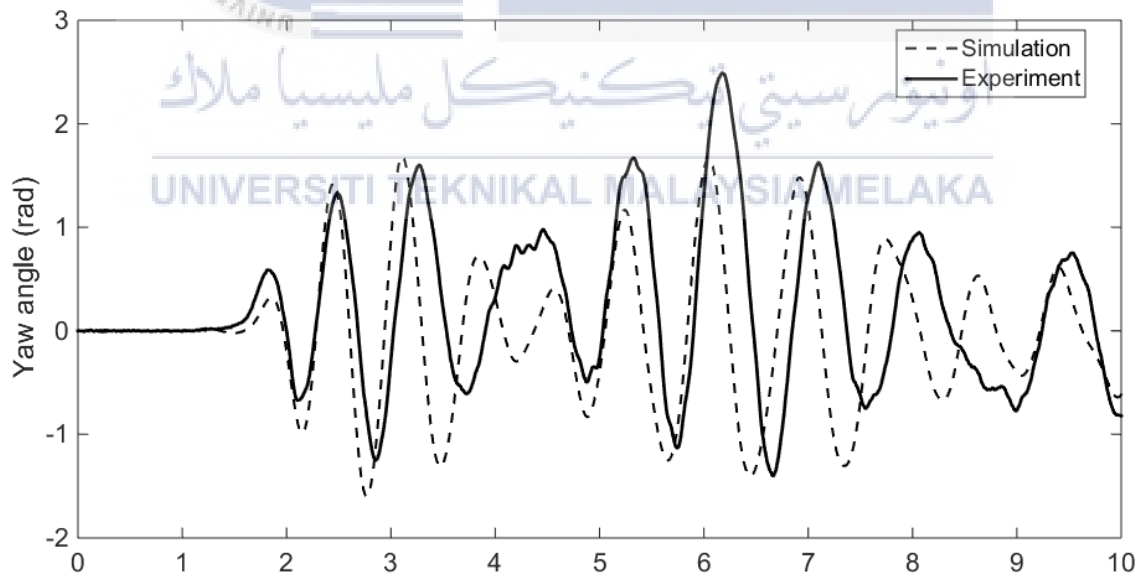Figure 4. 18 : Acceleration versus Time

Figure 4. 19 : Yaw angle versus Time
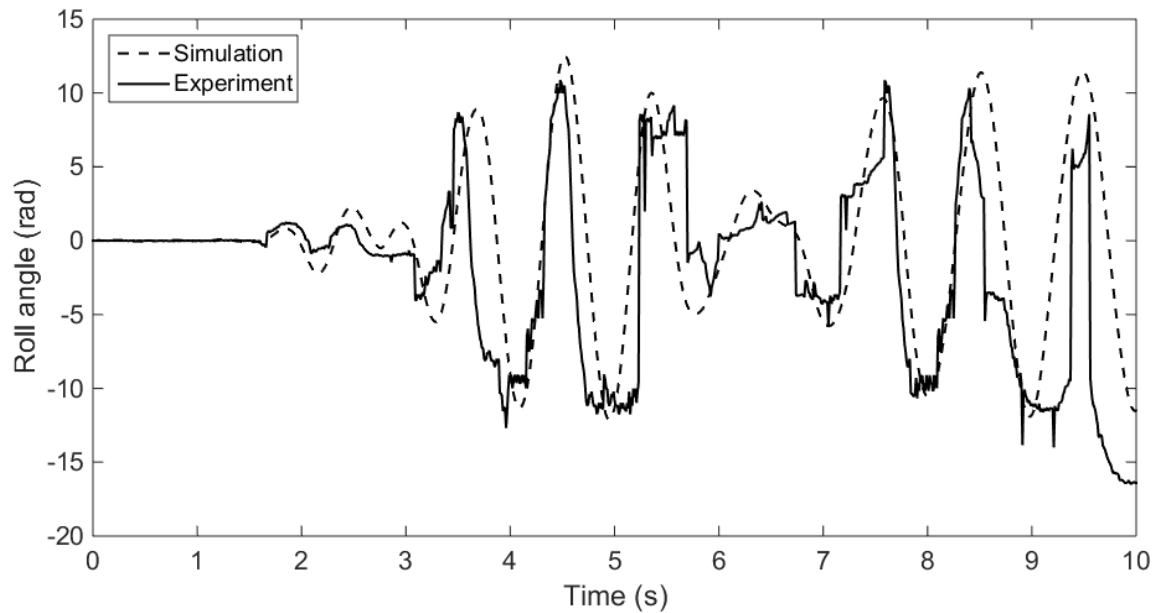
Figure 4. 20 : Roll angle versus Time

Figure 4.18 shown the validation result of the acceleration versus time from the simulation and experiment. We can see the pattern of the acceleration were linked to the different model between simulation and also experiment. The pattern through experiment were a bit fuzzy and close but when validate with the simulation pattern, it almost same. The amplitude of simulation graph were high at the 3 to 6 second. It's due to the assumption that already mentioned earlier at the chapter 3. There are some dimension that already assume to the constant value. But in the experiment, all the dimension consider were random and some of them that consider in experiment had already been assumed in simulation. Then, the graph gradually same each other. The highest amplitude that recorded for simulation and experiment were between $0.4 \ m/s^2$ and $0.5 m/s^2$.

62

The yaw angle of the motion also been considered in the validation. In figure 4.19, the yaw angle of simulation and experiment has been estimated. Here the rotational distance were mentioned in "radian" is varied by time factor in "second". There is a little bit visible difference between these curves as they travel parallel to each other by a small space. Both curves were travel at the same pattern. Both start at the zero angle for 2 second and gradually increase and decrease the value of angle. The experiment show slightly higher value of yaw angle than simulation at 6 second. The graph were slightly difference at 4 to 5 second as the experiment result increase but simulation were decrease. It may because of the moment of the inertia that had been considered in the experiment.

In figure 4.20, the roll angle of simulation and experiment also had been estimated. Here the rotational distance were mentioned in "radian" is varied by time factor in "second". We can see both curves were travel parallel to each other but there is different of the curves. The simulation curves were plotted smoothly but for the experiment curves, there is an irregularities due to the random input. So the graph of the experiment were not smooth as simulation curves. The curves were still valid as the pattern were same and parallel to each other.

CHAPTER 5

CONCLUSION AND RECOMMENDATIONS

In conclusion, this paper present a dynamic modelling for the full railway vehicle model. A full railway vehicle model with 17 DOF were described to represent the railway vehicle lateral model. 17 equation also were described including bogie dynamic, wheel set dynamic, and also vehicle body dynamic. This paper contain of two part that is simulation and experiment. The study used MATLAB-Simulink as a medium to simulate the dynamic behavior and also evaluate the performance of the model. The simulation study were performed with determined the dimensional analysis of the scaling method. To make sure the simulation were performed smoothly, a few assumption were defined according to the stage of the simulation. Four scaling method were introduced in this paper that is Pascal, Jaschinski, Iwnicki and Jaschinski Modified Method. The scaling factor for each method were used to get the dimensional analysis and were described in chapter 3. With the simulation that had been done, I can compare how the pattern for each of the scaling method with the real scale. The result were demonstrated in the graph form of time response of displacement, acceleration, yaw and roll to differentiate of each scaling method. Then, the most valid scaling strategy were chosen to for the validation.

Besides that, the Test Rig were introduced as one of the main objectives in this paper. The mechanism were fabricated to push and pull the test rig on the lateral motion to get the result for the validation. The LVDT, gyro sensor and accelerometer sensor were used in the experiment to obtained the acceleration, yaw and roll result for the experiment. On top of that, the simulation and experiment result were validate to analysis each of the result as the random

input were given by the experiment. The validation were valid for each result and the objective for this paper were achieved. The model in the simulation match well with the experiment model and can be used for future study.

As a recommendation for the future study, the implementation for the control that provide an improvement to vehicle dynamic performance. As for this paper, the simulation that used for the real lateral motion were valid and can implement any control in it to improve the performance before testing it to the real scale of railway vehicle. Next, recommend to study the simulation of scaling method in different track of irregularities to improve the performances of the control and the implementation in the simulation.

REFERENCES

Baiasu, D., Ghita, G., & Sebesan, I. (2013). Control system with magnetorheological fluid device for mitigation of the railway vehicle hunting oscillations. *Journal of Physics: Conference Series*, *412*(1). https://doi.org/10.1088/1742-6596/412/1/012043

Bian, X., Jiang, H., Chang, C., Hu, J., & Chen, Y. (2015). Track and ground vibrations generated by high-speed train running on ballastless railway with excitation of vertical track irregularities. *Soil Dynamics and Earthquake Engineering*, *76*, 29–43. https://doi.org/10.1016/j.soildyn.2015.02.009

Dahlberg, T. (2006). Handbook of Railway Vehicle Dynamics. https://doi.org/10.1201/9781420004892

Eickhoff, B. M., Evans, J. R., & Minnis, A. J. (1995). A Review of Modelling Methods for Railway Vehicle Suspension Components. *Vehicle System Dynamics*, *24*(6–7), 469–496. https://doi.org/10.1080/00423119508969105

Grant, C., Love, I., Millner, D., Chiles, N., Deandrea, W. L., Craig, E., … Johnson, N. (2012). Gaysia : Adventures in the Queer East , 2012 , 276 pages , Benjamin Law , 1921870745 , (March 2009). https://doi.org/10.1201/9780849333217

Hudha, K., Harun, M. H., Harun, M. H., & Jamaluddin, H. (2011). Lateral suspension control of railway vehicle using semi-active magnetorheological damper. *IEEE Intelligent Vehicles Symposium, Proceedings*, (Iv), 728–733. https://doi.org/10.1109/IVS.2011.5940544

Islamic, I. (2016). Mathematical Modeling and Control of Active Suspension System for a

Quarter Car Railway Vehicle, *10*, 227–241.

Iwnicki, S. D., & Wickens, A. H. (1998). Validation of a MATLAB railway vehicle simulation using a scale roller rig. *Vehicle System Dynamics*, *30*(3–4), 257–270. https://doi.org/10.1080/00423119808969451

Ji, H., Yamada, M., Hsu, S., & Kulsrud, R. (1998). Experimental Test of the Sweet-Parker Model of Magnetic Reconnection, 13–16.

Koch, G., Pellegrini, E., Spirk, S., & Lohmann, B. (2010). Design and modeling of a quarter-vehicle test rig for active suspension control. *Technische University at München*, *5*(1), 1–28.

Ma, X. N., & Yang, S. P. (2008). Self-adapt fuzzy control of a semi-active suspension of high-speed locomotive with MR dampers. *Proceedings of the 7th International Conference on Machine Learning and Cybernetics, ICMLC*, *4*(July), 2120–2124. https://doi.org/10.1109/ICMLC.2008.4620756

Metin, M., & Guclu, R. (2011). Active vibration control with comparative algorithms of half rail vehicle model under various track irregularities. *JVC/Journal of Vibration and Control*, *17*(10), 1525–1539. https://doi.org/10.1177/1077546310381099

Naeimi, M., Li, Z., Dollevoet, R., & Law, A. S. (2014). Scaling Strategy of a New Experimental Rig for Wheel-Rail Contact, *8*(12).

Polach, O., Berg, M., & Iwnicki, S. (2006). Oldrich Polach, Mats Berg, and Simon Iwnicki.

Politecnico, M. (2000). Simulation of a scaled roller rig. *Meccanica*, 1–10. https://doi.org/10.1016/j.bmc.2010.01.055

Shen, Y., Yang, S., & Yin, W. (2006). Application of magnetorheological damper in vibration control of locomotive. *Proceedings of the World Congress on Intelligent Control and Automation (WCICA)*, *2*(1), 8113–8116. https://doi.org/10.1109/WCICA.2006.1713554

Shimamune, R., & Tanifuji, K. (1995). Application of oil-hydraulic actuator for active suspension of railway vehicle: experimental study. *SICE '95. Proceedings of the 34th SICE Annual Conference. International Session Papers*, 1335–1340. https://doi.org/10.1109/SICE.1995.526705

Wickens, A. H. (2006). A History of Railway Vehicle, 5–38.

Zhou, R., Zolotas, A., & Goodall, R. (2011). Integrated tilt with active lateral secondary suspension control for high speed railway vehicles. *Mechatronics*, *21*(6), 1108–1122. https://doi.org/10.1016/j.mechatronics.2011.07.001

 C. Esveld, "Modern railway track", Second ed., MTR-Productions, Zaltbommel, The Netherlands 2001.

C. Heliot, "Small-scale test method for railway dynamics", Vehicle System Dynamics, vol. 15 (1986) pp. 197-207.

Craftman, 2016. Model train scale and gauge (online)

Available at: http://rrmodelcraftsman.com/model-train-scale-gauge/

Micro-mark, n.d. history of model train scales

Available at: https://blog.micromark.com/history-of-model-train-scales/

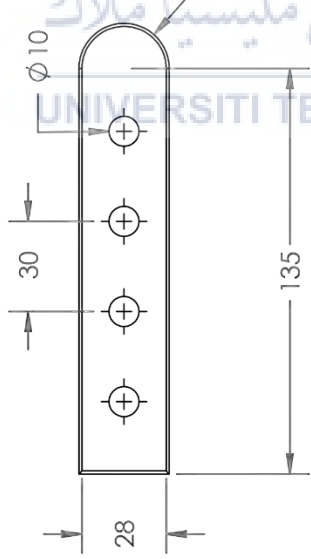Oda, N., N. S. (1970). Vibration of air suspension bogies and their design. Bulletin of JSME, 13(55)

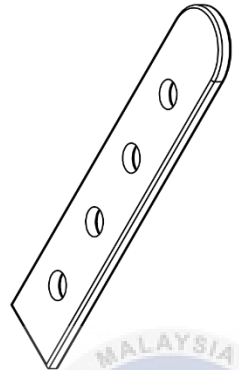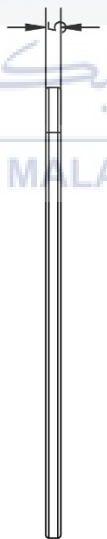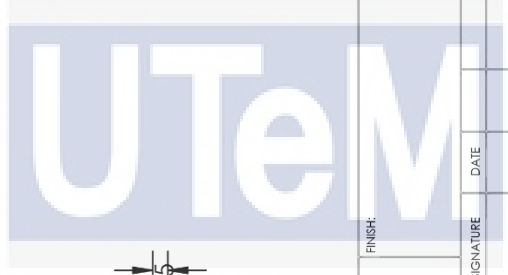| NO	TASK	W1	W2	W3	W4	W5	W6	W7	W8	W9	W10	W11	W12	W13	W14
1	Approval from supervisor and register for the project title	▓									▓				
2	Discussion about details of the project		▓								▓				
3	Planning on the meeting and briefing about PSM 1			▓							▓				
4	study about MATLAB and research about the parameters				▓						▓				
5	Reference and the literature review		▓							▓	▓	▓			
6	Identify the parameters used										▓				
7	Using MATLAB to do the simulation on the parameters								▓		▓				
8	Progress report and submit								▓		▓				
9	Chapter 2: literature review									▓	▓	▓			
10	Chapter 3: methodology										▓	▓			
11	Compilation of PSM 1 final report										▓		▓		
12	Presentation of PSM 1										▓			▓	
13	Submit final report PSM 1										▓				▓

NO	TASK	W1	W2	W3	W4	W5	W6	W7	W8	W9	W10	W11	W12	W13	W14
1	Discussion about comment and mistakes in PSM 1 report	■								███					
2	Brainstorming about improvement on the report.		■							███					
3	Discussion about the test rig and the improvement for it.			■	■					███					
4	Research and study about the test rig and the mechanism					■	■	■		███					
5	List out and design the suitable mechanism							■	■	███					
6	Prepare progress report and submit for the result of the simulation								■	███					
7	Fabrication of the mechanism									███	■	■	■		
8	Test on the Test Rig									███				■	
9	Validation of the simulation									███			■	■	
10	Prepare chapter 4 and chapter 5 and present to supervisor									███				■	
11	Compilation of PSM 2 final report									███				■	
12	Presentation of PSM 2									███					■
13	Submit final report PSM 2									███					■

70

Short Steel

R15
Ø10
30
135
28

DEBUR AND
BREAK SHARP
EDGES

DO NOT SCALE DRAWING

REVISION

FINISH:

UNLESS OTHERWISE SPECIFIED:
DIMENSIONS ARE IN MILLIMETERS
SURFACE FINISH:
TOLERANCES:
   LINEAR:
   ANGULAR:

NAME   SIGNATURE   DATE

DRAWN
CHK'D
APPV'D
MFG
Q.A

TITLE:

Short Steel

MATERIAL:

WEIGHT:

DWG NO.

SCALE:1:2

SHEET 1 OF 1

A4

Bearing

35
Ø26
10
60
80
20
Ø26
Ø5

UNLESS OTHERWISE SPECIFIED:
DIMENSIONS ARE IN MILLIMETERS
SURFACE FINISH:
TOLERANCES:
   LINEAR:
   ANGULAR:

FINISH:

DEBUR AND
BREAK SHARP
EDGES

DO NOT SCALE DRAWING   REVISION

	NAME	SIGNATURE	DATE
DRAWN			
CHK'D			
APPV'D			
MFG			
Q.A			

TITLE:

MATERIAL:

DWG NO.

WEIGHT:

A4

SCALE:1:1   SHEET 1 OF 1

Long steel

UNLESS OTHERWISE SPECIFIED:
DIMENSIONS ARE IN MILLIMETERS
SURFACE FINISH:
TOLERANCES:
   LINEAR:
   ANGULAR:

DEBUR AND
BREAK SHARP
EDGES

FINISH:

DO NOT SCALE DRAWING

REVISION

NAME | SIGNATURE | DATE

DRAWN
CHK'D
APPV'D
MFG
Q.A

TITLE:

MATERIAL:

WEIGHT:

DWG NO.

A4

SCALE:1:5

SHEET 1 OF 1

Ø20
Ø10
Ø26

50
330
35
35

Steel Plate

Dimensions shown on drawing: Ø33, Ø13, 50, 50, 62.50, 2.50

Short Nut

4.50

19.50

17.32

Ø10

75

Motor

142.50

110

10

Ø26

Ø10

R32.50

30

19

UNLESS OTHERWISE SPECIFIED:
DIMENSIONS ARE IN MILLIMETERS
SURFACE FINISH:
TOLERANCES:
LINEAR:
ANGULAR:

DEBUR AND
BREAK SHARP
EDGES

DO NOT SCALE DRAWING | REVISION

FINISH:

NAME | SIGNATURE | DATE

DRAWN
CHK'D
APPV'D
MFG
Q.A

TITLE:

MATERIAL:

WEIGHT:

DWG NO.

A4

SCALE:1:2 | SHEET 1 OF 1

ITEM NO.	PART NUMBER	QTY.
1	Bearing	1
2	motor	1
3	Long Steel	1
4	nut long	1
5	Short Steel	1
6	nut	3
7	Steel plate	1
8	nut short	1

SCALE 1 : 3

77